European Journal of Agronomy 101 (2018) 222–238

Contents lists available at ScienceDirect

European Journal of Agronomy

journal homepage: www.elsevier.com/locate/eja

Climate change impacts on agro-climatic indices derived from downscaled weather generator scenarios for eastern Denmark

Signe B. Rasmussen[a,*], Stephen Blenkinsop[b], Aidan Burton[b], Per Abrahamsen[a], Peter E. Holm[a], Søren Hansen[a]

[a] Department of Plant and Environmental Sciences, University of Copenhagen, Thorvaldsensvej 40, 1871 Frederiksberg C, Denmark
[b] School of Engineering, Newcastle University, Newcastle upon Tyne, NE1 7RU, UK

ARTICLE INFO

Keywords:
Hourly rainfall
RainSim
Statistical change factors
Subsurface drainage
Crop water shortage
Field trafficability

ABSTRACT

The agricultural sector supports the growing world population with food and successful crop production is highly dependent on the prevailing climatic conditions. A modelling analysis of projected future changes in agroclimatic conditions is presented for eastern Denmark, focussing on indices of drainage need, field trafficability, water shortage and relative production (the ratio between actual and potential production). Projected climatic change from 11 climate model simulations were downscaled by perturbing a weather generator calibrated on meteorological data (hourly rainfall and daily air temperature, wind speed, sunshine hours, relative humidity), from a location in eastern Denmark. The analysis was carried out for the control period (1983–2012), the near future (2030–2059) and the far future (2070–2099). 3000 year long weather series were generated for each period and used to drive the agro-ecological model, Daisy. The Daisy model setup included two structurally different soils and two crops.

Silage maize was found to benefit from the longer potential growing season in the future, but it is likely that the unchanged or slightly decreased summer rainfall will not be sufficient to meet the increased water requirements and irrigation might be necessary to reach the production potential. The winter wheat cultivar used in the analysis was found to have a shorter active growing season in the future, and so yields actually reduced. The effects of increased winter rainfall do not show a clear change in trafficability, but mean drainage flow increased by an average of 10% in the near future and 16% in the far future. Thus, the results suggest a potential for increased future crop production in eastern Denmark, however the choice of crops and cultivars needs consideration, and maintenance of the drainage system should also be a priority.

1. Introduction

The effects of climate change on crop and terrestrial food production have already become evident in several regions of the world over the past half century, leading to a reduction in wheat and maize production for many regions (Porter et al., 2014). Further, for the major crops in many areas it is expected that climate change will have a detrimental impact on yields (Zhao et al., 2017), with Asseng et al. (2014) estimating that global wheat production could fall by 6% for each °C of future temperature increase, and become increasingly variable over space and time, although some locations may benefit (Easterling et al., 2007; EEA, 2017). In Scandinavian countries, like Denmark, the future growth of grain crops is expected to increase due to the higher temperatures and atmospheric CO_2 levels, as the active growth starts earlier and crops develop faster (Olesen et al., 2006).

Agricultural crop production is generally constrained by temperature, incoming solar radiation, and water and nutrient supply (Reyer et al., 2013). In Scandinavian countries like Denmark, mean temperature mainly affects the length of the growing season, but radiation as well as late spring and early autumn frost may also limit the growing season. For example, in Germany the growing season is 1–3 months longer than in Scandinavian countries (Mela, 1996).

Current crop production in Nordic European countries is usually rain fed with rainfall effects on plant growth expressed either as scarcity which results in drying and wilting, or as water excess leading to e.g. stunted root growth (Reyer et al., 2013). A window of perfect soil water content for plant growth is additionally dependent on soil properties, such as soil texture and soil organic carbon content with irrigation

* Corresponding author.
E-mail addresses: sbra@plen.ku.dk (S.B. Rasmussen), stephen.blenkinsop@ncl.ac.uk (S. Blenkinsop), aidan.burton@ncl.ac.uk (A. Burton), pa@plen.ku.dk (P. Abrahamsen), peho@plen.ku.dk (P.E. Holm), sha@plen.ku.dk (S. Hansen).

https://doi.org/10.1016/j.eja.2018.04.004
Received 27 October 2016; Received in revised form 1 April 2018; Accepted 11 April 2018
Available online 23 October 2018
1161-0301/ © 2018 Published by Elsevier B.V.

mainly restricted to coarse sandy soils or similar, which may experience water scarcity during summer (Aslyng, 1978). Water excess is a more common issue in the Nordic countries, which may be overcome through the use of artificial drainage. In Denmark 50–60% of the agricultural land is artificially (subsurface) drained (Olesen, 2009) as an excess of soil water may result in postponed sowing of the fields in spring, due to poor ability of the soil to support increasingly large and heavy farming machinery. Furthermore, root growth is restricted, which causes a higher risk of drought damage during summer time. Additionally, soils suffering from water excess may increase the risk of soil erosion (Panagos et al., 2015), lodging (Niu et al., 2016), and transportation of agrochemicals to surface waters (Flury, 1996; Rasmussen et al., 2015). Wet conditions also favour many weed species, which increases the need for mechanical and chemical weed control.

Besides mean annual or seasonal rainfall, extreme rainfall events also pose a challenge to crop production. Effects of extreme rainfall events include increased risk of lodging (Niu et al., 2016), crusting of the soil surface prior to seed germination (which makes it hard for the sprout to penetrate the soil surface), or soil erosion before seed germination (which causes physical transportation/relocation of seeds), (Håkansson et al., 2012; Panagos et al., 2015). Additionally, intense rainfall may cause a rapid transport of agrochemicals, such as nutrients and pesticides, via preferential flow pathways to tile drains, posing an environmental threat to the aquatic environment (Kjaer et al., 2011). Heavy rainfall events capable of triggering such processes are most often characterised as sudden, intense events, with high variability at hourly temporal resolution (Rasmussen et al., 2015).

The European Union funded project ENSEMBLES (van der Linden and Mitchell, 2009) projected that climate change in northern Europe will result in increased mean temperature, winter rainfall, and frequency of extreme weather events. These statements are supported by more recent general circulation model (GCM) projections based on the IPCC Fifth Assessment Report (IPCC, 2014),[1] where Denmark is projected to experience an annual increase in air temperature of between 1.2 and 3.7 °C (depending on emissions scenario) by the end of this century (Olesen et al., 2014). Hence, it is likely that the local temperature will increase by more than 2 °C which has been suggested as a threshold between future increases and decreases in crop production in many regions (Easterling et al., 2007). However, Challinor et al. (2014) indicated that adaptation losses in crop production might be expected by 2 °C of local warming. Projected changes in rainfall show a clear seasonal dependence, where autumn, winter and spring are expected to experience increased rainfall, and summer decreased rainfall (van der Linden and Mitchell, 2009). By use of the latest RCP scenarios annual rainfall in Denmark is expected to increase by between 1.6 and 6.9%, by the end of this century (Olesen et al., 2014). Extreme rainfall events have not yet been analysed for Denmark based on the RCP-scenarios, but it is expected that the previously projected trends will continue (Olesen et al., 2014).

Numerous studies have investigated the direct effect of changed climate on crop growth and yield (e.g. Gobin 2010; Grass et al., 2015; Doltra et al., 2014; Vanuytrecht et al., 2014; EEA, 2017). As winter wheat is an important crop in Denmark, substantial research has been undertaken on the effects of climate change on Danish winter wheat yields (e.g. Martin et al., 2014; Patil et al., 2012). However, the majority of these studies were conducted using crop yield models driven by downscaled climate model output and assuming present crops and agricultural practice in the future. These assumptions are problematic as both cultivars and agricultural practices adapt to climatic changes over time. Rather than trying to predict absolute yield changes on the basis of present or future management and cultivars, we use an approach based on changes in the *conditions* for agriculture, such as the length of the growing season and the need for irrigation and subsurface drainage.

[1] https://www.ipcc.ch/report/ar5/wg1/.

A previous study by Trnka et al. (2011) investigated projected changes in agroclimatic conditions at the European level, but concluded that such an analysis should also be conducted at a regional and local level, to better reflect potential future challenges related to climate change. Trnka et al. (2011) used a pattern scaling approach applied to a weather generator to downscale three GCM projections. Here, the work by Trnka et al. (2011) is advanced by conducting a similar analysis at a smaller scale (eastern Denmark), using four GCM projections, using RCMs to dynamically downscale these projections (totalling 11 GCM*RCM pairings) and using a sophisticated change factor plus weather generator methodology to produce control and future downscaled weather scenarios. The present work applies a physically based complex soil-water-atmosphere model and corresponding realistic parameterizations of two agricultural soil types providing the possibility of evaluating changes in subsurface drain flow (Mollerup et al., 2014). Potential change in extreme rainfall indices at hourly resolution were also added to this analysis, providing new information on the magnitude of challenges crop production will face as a consequence of these events. Running the simulations at hourly resolution for rainfall as opposed to daily values improves the simulation of the soil water dynamic, including activation of preferential flow pathways as well as the distribution between evaporation from free water surfaces and transpiration through the stomata. Furthermore, grid averages (25*25 km) provided by the RCMs are spatially too coarse to properly simulate the fine-scale processes mentioned above. Hence, spatial downscaling is also necessary.

To evaluate future changes of agro-climatic conditions in Denmark, stochastic simulations of precipitation, air temperature, wind speed, humidity and global radiation were downscaled from RCM output for the periods 1983–2012 (control), 2030–2059 (near future) and 2070–2099 (far future). Time series were produced by the stochastic rainfall model RainSim V3 (Burton et al., 2008), and the Climatic Research Unit (CRU) weather generator (WG) (Kilsby et al., 2007; Watts et al., 2004; Jones et al., 2016), by applying statistical change factors (CFs) (Prudhomme et al., 2002), derived from the ENSEMBLES project (van der Linden and Mitchell, 2009). The simulated weather series were analysed for extreme events and general climatic indices, but were also used as input to the soil-plant-atmosphere model, Daisy (Hansen et al., 2012). Daisy simulated the field water balance for two different soil types, and under two different cropping systems (a spring sown crop and an overwintering crop). Potential future changes in management activities, such as sowing/harvesting dates, number of trafficable days, and drainage need, were evaluated together with changes in water shortage. This evaluation of future drainage needs particular attention, since there appear to be no published material on this matter. By combining the high resolution downscaled projections with the modelling approach we therefore aim to improve the combined understanding of the direct (e.g. temperature and rainfall) and indirect (e.g. need of irrigation and subsurface drainage) effects of climate change on conditions for agricultural crop production.

2. Material and methods

2.1. Meteorological data

To calibrate the weather generator, observed weather series with ideally a minimum length of 30 years are needed. The observed weather data used in this study, consisted of *daily* minimum and maximum temperature, wind speed, relative humidity (vapour pressure) and sunshine hours, combined with *hourly* precipitation values. The daily weather data covering the period from 1983 to 2012 originated from Copenhagen Airport (55°37′05″N 12°39′03″E), Denmark, and was provided by The Danish Meteorological Institute (DMI). Hourly rainfall data from a different measuring network (DWPCC, 2016) was available for the same 30 year period, and was included to incorporate changes in extreme short-duration rainfall events in the analysis. The choice of

study location was limited since Copenhagen Airport is the only location in eastern Denmark where both hourly rainfall and daily weather observations are available covering a period of 30 years.

2.2. Climate model projections

The ENSEMBLES project offers a series of control and future simulations of the European climate, using the SRES A1B (medium), emissions scenario (van der Linden and Mitchell, 2009). These simulations have been dynamically downscaled from coarse resolution GCMs using an ensemble of RCMs. Such multi-model ensembles reflect the uncertainty arising from different climate model structures, but not that associated with model parameterization which may alternatively be addressed by perturbed physics ensembles (Murphy et al., 2014). A truly comprehensive assessment of uncertainty should take into account the "cascade of uncertainty" referred to by Schneider (1983), additionally incorporating, for example, uncertainty arising from the future response of biogeochemical cycles and from the trajectory of emissions. The ENSEMBLES database is maintained and hosted by the Danish Meteorological Institute, and is accessible from the project homepage.[2] To represent climate model uncertainty in this study, an ensemble of 11 climate model simulations were investigated. Climate models were selected based on the following criteria to obtain a consistent group of projections: selection of the highest resolution (25 km), longest simulations (1951–2100), and consistent climate sensitivity to atmospheric CO_2 (excluding the low and high sensitivity Hadley GCMs). This resulted in eleven model pairings from four GCMs and eight RCMs for use in this study (Tables 1 and 2).

2.3. Deriving and applying change factors from regional climate models

The change factor (CF) method (e.g. see Jones et al., 2016 for details) applies the change signal from each member of an ensemble of climate model simulations, quantified as a set of monthly CFs, as an additive (or multiplicative as appropriate) perturbation to the observed climate statistics, under the assumption that climate model biases are consistent between control and future simulations. This yields an estimated climatology for the downscaled projected future scenario and time slice.

For each of the 11 selected GCM*RCM model pairings, simulated values of daily total precipitation and daily mean temperature were extracted, covering the control period (1983–2012), the near future (2030–2059), and the far future (2070–2099). RCM data were extracted from the 25*25 km grid cell overlying the meteorological station and the 8 surrounding grid cells. The climate simulations from all 9 grid cells in this 3*3 matrix, were compared in order to test the robustness/stability of the climate change signal. For temperature, a clear grouping of grid cells was identified for all 11 ensemble models in terms of their ability to reproduce observations (Fig. 1) which depended on whether they were classed as land or sea. Fig. 1 illustrates the grouping of grid cells between land and sea for the ECHAM-HIRHAM model pairing. Therefore, the grid cells considered as sea by the climate models were excluded and an average of CFs from those over land was calculated and used in the subsequent work. The rainfall signal also showed a grouping for some of the models (Fig. 2), but to maintain a consistency in the methodology, grid cells over sea were excluded for all models, as for temperature.

The following monthly change factors were calculated, representing climate model simulated change for the near and far future relative to the control period for each GCM-RCM pairing:

- mean and variance of temperature.
- mean, variance, skewness, lag-1 autocorrelation and proportion of dry days (PDD; days with less than 0.2 mm) for rainfall.

[2] http://ensemblesrt3.dmi.dk/.

Table 1
GCMs and RCMs from the ENSEMBLES project used in this study.

Climate model	Organisation	Reference
GCM		
Arpege	National Centre of Meteorological Research, France	Déqué et al. (1994)
BCM2	Bjerknes Centre for Climate Research, Norway	Otterå et al. (2009)
ECHAM5	Max Planck Institute of Meteorological Research, Germany	Roeckner et al. (2003)
HadCM3	Met Office Hadley Center, UK	Collins et al. (2006)
RCM		
CLM	Swiss Federal Institute of Technology Zurich, Switzerland	Böhm et al. (2006)
HadRM3	Met Office Hadley Center, UK	Jones et al. (2003)
HIRHAM5	Danish Meteorological Institute, Denmark	Christensen et al. (2006)
RACMO2	Royal Netherlands Meteorological Institute, Netherlands	Van Meijgaard et al. (2008)
RCA3	Swedish Meteorological and Hydrological Institute	Kjellström et al. (2005)
RegCM3	International Centre for Theoretical Physics, Italy	Pal et al. (2007)
Remo	Max Planck Institute of Meteorological Research, Germany	Jacob et al. (2001)
RM5.1	National Centre of Meteorological Research, France	Radu et al. (2008)

Table 2
Matrix of GCM*RCM pairings from the ENSEMBLES project used in this study.

		GCM			
		HadCM3	ECHAM5	Arpege	BCM2
RCM	HadRM3	X			
	Remo		X		
	RM5.1			X	
	HIRHAM5		X	X	X
	CLM	X			
	RACMO2		X		
	RegCM3		X		
	RCA3		X		X

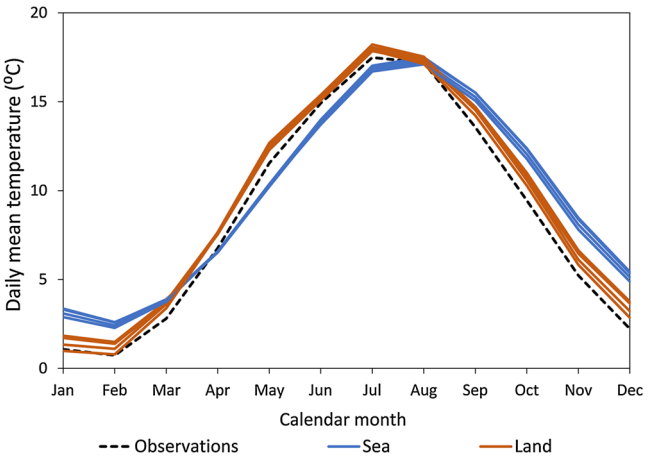

Fig. 1. RCM reproduction of observed daily mean temperature, from the ECHAM-HIRHAM pairing. Simulations from the 9 grid cells centred on the meteorological station are compared to observations. Blue lines represent grid cells located over sea, and brown lines represent grids located over land. (For interpretation of the references to colour in this figure, the reader is referred to the web version of this article.)

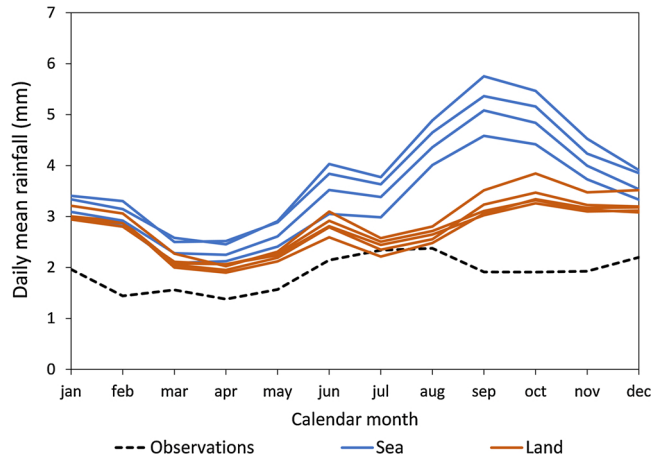

Fig. 2. RCM reproduction of observed daily mean rainfall, from the ECHAM-HIRHAM pairing. Simulations from the 9 grid cells centred on the meteorological station are compared to observations. Blue lines represent grid cells located over sea, and brown lines represent grid cells located over land. (For interpretation of the references to colour in this figure, the reader is referred to the web version of this article.)

The change in mean temperature is calculated as the difference between the future and control periods and is applied as an additive CF to perturb the climatology of the observations. CFs for the mean, variance and skewness of rainfall are calculated as the ratio of the future to the control statistic (and are applied as multiplicative CFs). This approach is also used for the calculation and application of the temperature variance CF. The rainfall PDD takes values within a limited range (0–1) and so it was first transformed using a simple invertible transformation, $X(\,)$, (e.g. see Jones et al., 2016) prior to the evaluation and application of a multiplicative CF.

Since RCMs do not typically provide information of the future weather at hourly resolution, CFs for hourly rainfall cannot generally be calculated directly from RCM outputs in the same way as for daily statistics. However, building on results by Cowpertwait et al. (1996, Section 4), Jones et al. (2009) presented a regression based methodology to estimate hourly variance and proportion dry from daily properties. The assumption that such relationships remain unchanged in the future allows the estimation of the future hourly rainfall statistics from the daily future statistics. Here, a linear regression analysis found useful relationships to estimate the hourly proportion dry (PDH), variance and skewness from the equivalent observed daily statistic (Fig. 3). These fitted relationships may then be applied to the control and estimated future daily properties of each statistic, g, to yield an expression of its hourly change factor, $\alpha_{g,H}$. So for the variance and skewness statistics:

$$\alpha_{g,H} = \frac{g_H^{Fut}}{g_H^{Ctrl}} = \frac{f_g(\alpha_{g,D}\ g_D^{Ctrl})}{f_g(g_D^{Ctrl})} \tag{1}$$

where the D and H suffixes indicate daily and hourly properties respectively, $\alpha_{g,D}$ is the daily change factor, the fitted regression in each case is $g_H = f_g(g_D)$, *Ctrl* and *Fut* indicate Control and Future respectively. The approach for the PDD and PDH statistics must however take account of the transformation and its inverse, $X(\,)$ and $X^{-1}(\,)$ respectively:

$$\alpha_{g,H} = \frac{X(g_H^{Fut})}{X(g_H^{Ctrl})} = \frac{X(f_g(X^{-1}(\alpha_{g,D}\ X(g_D^{Ctrl}))))}{X(f_g(g_D^{Ctrl}))} \tag{2}$$

Lag-1 autocorrelation is typically used in model fitting and simulation of rainfall but the relationship between the daily and hourly statistics was found to be poor ($R^2 = 0.14$). Given the lack of a robust relationship with which to estimate future hourly lag-1 correlation the control period values were assumed unchanged in the future scenarios. Application of the calculated CFs in order to produce the downscaled weather series are described in the subsequent step.

Hourly stochastic simulations of control period rainfall were generated using the stochastic rainfall model RainSim V3 (Burton et al., 2008). This is a Neyman-Scott Rectangular Pulses (NSRP) model (Cowpertwait et al., 1996), a Poisson cluster approach whereby storms occur as a Poisson process in time. Simulated rainfall time series consist of random clusters of rain cells, with intensity and duration properties, which combined make up a complete rainfall event. Further details of the model may be found in Burton et al. (2008) and Burton et al. (2010). RainSim was initially calibrated using the observed hourly precipitation series. One hundred 30-year long hourly resolution simulations possessing the same statistical properties as the observations (control period) were used to evaluate the performance of the model. The ability of RainSim in reproducing observed rainfall statistics (hourly mean, daily lag-1 autocorrelation, daily and hourly skewness and variance, together with PDD and PDH) was evaluated and found to have adequate skill. Thereafter CFs derived from the RCM outputs were applied to the observed statistical properties to produce perturbed rainfall statistics for each of the future periods. These perturbed statistics were then used to calibrate the model, resulting in additional rainfall simulations representing the future climates. A 3000-year hourly rainfall simulation was then generated for each GCM*RCM pairing and future time-slice (22 datasets in total), along with a 3000-year control period scenario for comparison.

The remaining weather variables, *daily* temperature (mean, T_{max} and T_{min}), vapour pressure, wind speed and radiation, were modelled conditionally on the simulated rainfall using the Climatic Research Unit (CRU) weather generator (hereafter CRU WG) (Kilsby et al., 2007; Watts et al., 2004). The CRU WG stimulates daily mean temperature and daily temperature range by a first-order auto-regressive process incorporating the observed lag-1 daily mean temperature, temperature range and precipitation from the rainfall model (here aggregated to daily). Secondary weather variables may be simulated by means of regressive and auto-regressive relationships. The simulated variables were then used to calculate reference evapotranspiration (ET_0) using the Penman–Monteith method (FAO, 1986). Further details on the use of the CRU WG are provided by Kilsby et al. (2007) and Jones et al. (2009). Initially, 100*30-year *daily* time series of temperature (mean, T_{max} and T_{min}), vapour pressure, wind speed and radiation were generated at daily resolution for the control period, so that the model could be evaluated. This evaluation confirmed the ability of the model to reproduce annual cycles of both mean and variance of all WG variables (in the sense that the differences between characteristics derived from observed and simulated data were statistically insignificant and related mostly to the stochasticity of the generation process). Some statistically significant differences in ET_0 were noted in winter months but these should not significantly affect the subsequent Daisy simulation results. Next, daily resolution 3000-year future weather series were generated for each GCM*RCM pairing and future time slice, conditioned on the future rainfall series, generated by RainSim. A 3000-year control period scenario was also generated for comparison. The complete set of weather series, control and future simulations, therefore consists of downscaled hourly precipitation data generated by RainSim, accompanied by daily values of temperature, vapour pressure, wind speed and radiation generated by the CRU WG.

2.4. Daisy model setup and parameterization

The simulated weather data were analysed according to selected climatic indices, and used to run the soil-water-atmosphere model Daisy (Hansen et al., 2012). Daisy is a deterministic, dynamical 1D/2D model developed for simulating agro-ecological systems. It is commonly applied at field scale, but can also be integrated into a modelling framework that, for example, simulates hydrological processes at the catchment scale (Boegh et al., 2004). It simulates water, carbon, and

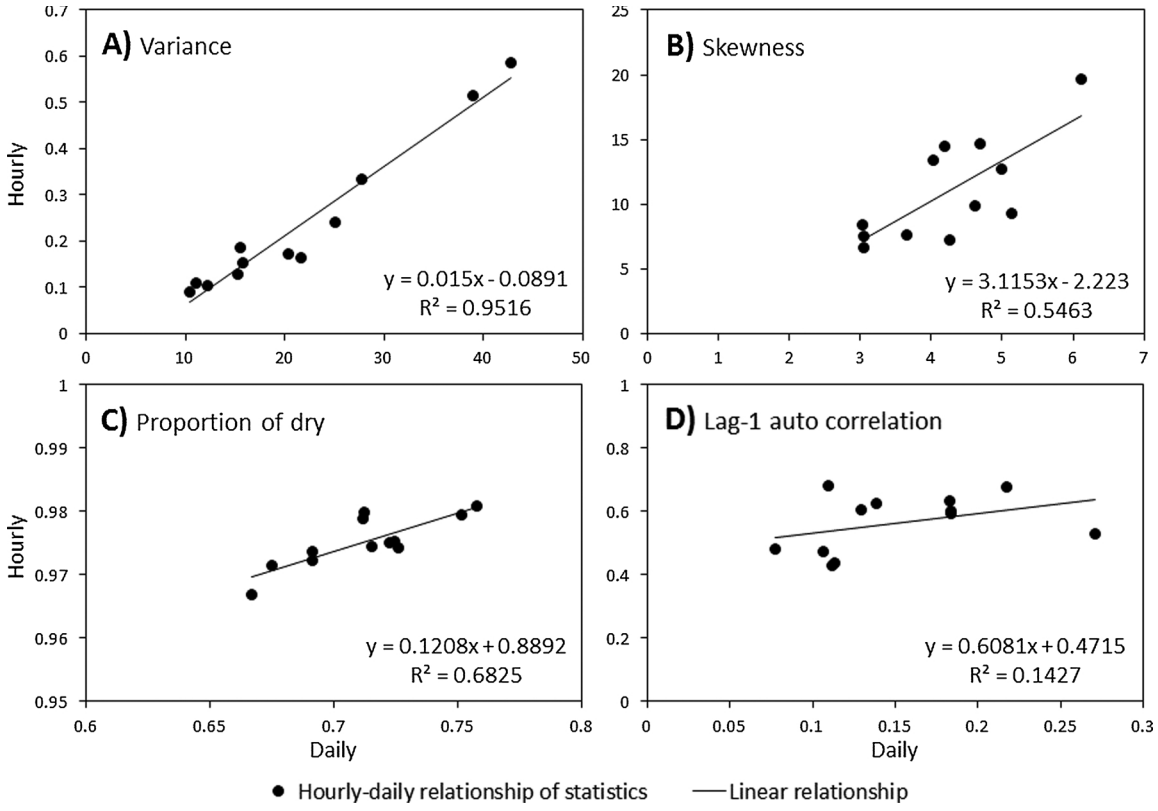

Fig. 3. Monthly relationships, between hourly and daily observed statistics, used for calculation of hourly change factors from daily change factors.

nitrogen balances and crop production under different agricultural management strategies (e.g., Gerke et al., 1999; Gjettermann et al., 2008; Andreasen et al., 2013). Furthermore, it can simulate the fate of fertilizers and pesticides (Hansen et al., 2012). To run the Daisy model, information on soil properties (e.g., texture and hydraulic properties), agricultural practice (e.g., crops, fertilization, pesticide application, irrigation, and tillage), and weather (e.g., precipitation, air temperature, air humidity, wind speed, and solar radiation) is required. Detailed simulations can be conducted when high resolution (hourly or finer) weather data are available (Rasmussen et al., 2015). Daisy is given reference evapotranspiration (ET_0) based on FAO (1986). This is used together with dynamic information about the canopy to calculate a crop specific potential evapotranspiration (*ETc*). Together with dynamic information about the soil water content, this is used for calculating the actual evapotranspiration (*ETa*), which is included in the final water balance for the system. If less detailed model output is needed, the model can be run at low resolution (daily time step) solely based on a minimal set of weather variables: precipitation, air temperature, and solar radiation. In this study, the simulations were run with hourly rainfall accompanied by daily values of air temperature, air humidity, wind speed, and solar radiation. The Daisy simulations included two typical crops grown for two different Danish agricultural soil types, hence four different model setups were applied. The simulations were used to evaluate potential differences in plant water deficiency, drainage need (for the sandy loam soil), number of field trafficable days (for the sandy loam soil), and dates for sowing and harvesting of crops.

The investigated soil types, coarse sand and sandy loam, were chosen to represent two typical agricultural soil types in Denmark. The coarse sandy soil is a homogeneous coarse textured soil with free drainage conditions, whereas the sandy loam is a heterogeneous soil containing several horizons, preferential flow pathways, subsurface drains and the hallmarks of long term agricultural use (a compaction layer of lower hydraulic conductivity is applied at the top of the B-horizon (B_{plow})). Both soils are modelled in 1D, and the parameterization is adopted from the study by Rasmussen et al. (2015). Standard soil characteristics are shown in Table 3.

Two crops, winter wheat (WW) and silage maize (SM), were chosen to represent a spring sown crop (silage maize), and an overwintering crop (winter wheat), both of which have a long growing season. The selected crops are considered important national and international crops (FAO, 2015), being cultivated in a range of different climates. It is expected that they will be present in future agricultural crop rotations in Denmark, and the use of maize is especially expected to increase (Elsgaard et al., 2012). The simulations here will not focus on specific crop yields (e.g. in tonnes), but will be used as an indicator of growth conditions. The crop model in Daisy is well tested, and both crops have successfully been simulated under Danish as well as other climates (e.g. Hansen et al., 1991, Kloss et al., 2012, Manevski et al., 2015, Palosuo et al., 2011, Svendsen et al., 1995). The ability of the crop models in Daisy in reproducing realistic crop yields and phenology (date of maturity/ready for harvest), were tested under current weather conditions and found satisfying.

Table 3
Soil characteristics for the two selected agricultural soil types, coarse sand and sandy loam, used in the Daisy simulations. Ksat indicates saturated hydraulic conductivity. Data originates from Jacobsen (1989) and Hansen et al. (2012).

Soil type	Horizon	Soil depth	Clay	Silt	Sand	Humus	Ksat
		cm	%	%	%	%	cm hour^{-1}
Coarse sand	Ap	0–30	3.8	7.2	86.7	2.3	21.7
	C	30–200	2.8	2.3	94.5	0.4	92.5
Sandy loam	Ap	0–25	10.4	21.6	65.1	2.9	0.17
	Bplow	25–33	14.6	21.1	62.8	1.6	0.05
	Bt	33–120	21.9	19.2	57.4	1.6	0.27
	C	120–200	20.5	23.3	55.2	1.0	1.50

For simplicity the sowing date of WW is kept constant (5th September) in all 3000 simulations, whereas the sowing date of SM is allowed to shift according to soil temperature. The sowing of SM depended on agro-climatic conditions, as it was set to occur when the soil temperature at 10 cm depth reached 10 °C (e.g. Olesen et al., 2000), but no later than July 1st. In the future warmer climate it is possible that farmers will sow WW later in the season, in order not to lose the cold tolerance of the crops. However, it is difficult to simulate such a response, as it depends on the weather to come (forecast) and not specific conditions of either soil or current weather. It was therefore decided to keep the sowing date of WW constant, although it means that possible negative effects of lost cold tolerance on crop yields are not included in the study. The harvesting of both crops occurred when the crop was ripe.

Both crops were simulated with unlimited nutrient supply to isolate the effect of climatic changes. Furthermore, the setups of the two crop systems were repeated with an additional assumption of unlimited water supply, which constitutes ideal conditions for crop growth and represents a production maximum. Comparing crop yields of simulations with unlimited water supply with simulations of realistic water supply, allows an evaluation of the state of future production potential regarding water availability. The 8 different setups (2 soil types and 2 crops under 2 water regimes), were simulated using the 23 3000-year-long weather series, corresponding to the control period and the 2 future time slices from the 11 GCM-RCM climate model pairs. This provided a total of 552,000 simulated growing seasons, giving a robust sample of potential changes.

2.5. Agro-climatic indices

Agro-climatic indices (Table 4) were chosen to characterize potential effects of changed climate on conditions for crop production and management in Denmark. The selected indices are inspired by those investigated by Trnka et al. (2011), however, they have been modified and supplemented in order to fit the specific purpose and methodology of this work. Specific novelties are the relative production potential and subsurface drainage need. The indices are furthermore divided into two groups: climatic indices which are solely conditioned by the weather (analysis of synthetic temperature and rainfall time series); and agro indices, concerning soil and crop responses to the weather (simulated by the Daisy model). The indices were calculated for each of the 3000 growing seasons, at monthly or annual resolution (as appropriate). From there the means and variability were calculated, enabling a comparison between the control and future periods to assess the impact of climate change.

Table 4
Investigated agro-climatic indices. All indices are calculated for each of the 3000 simulated growing seasons for each of the 23 climate scenarios, and from there an annual or monthly average is calculated.

Abbreviation	Description
Climatic indices	
FD	Frost days (number of days with air temperature < 0 °C. Annual)
DFAF	Date of first air frost (autumn, air temperature < 0 °C. Annual)
DLAF	Date of last air frost (spring, air temperature < 0 °C. Annual)
T_{COLD}	Coldest day of the year (°C, Annual)
T_{WARM}	Hottest day of the year (°C, Annual)
GROW	Length of potential growing season (number of days with daily mean temperature > 5 °C. Annual)
R_{med}	Median of monthly maximum 1 h rainfall (Monthly)
R_{maxH}	Greatest 1 h rainfall (mm h^{-1}. Monthly)
WD	Wet days (number of days with rainfall ≥ 10 mm. Monthly)
SDII	Simple daily intensity index (average intensity (mm day^{-1}) on rain days. Monthly)
Agro indices	
Water shortage	Potential evapotranspiration minus actual evapotranspiration (mm. Annual)
Relative production	Crop yield relative to yield when assumed no water shortage (%. Annual)
Sowing date	Of silage maize (restricted by soil temperature, Annual)
Harvest date	Of winter wheat and silage maize (when crops are ripe. Annual)
Trafficability	Number of field trafficable days (Soil water content in the top 10 cm $<$ Field capacity. Monthly)
Drainage volume	Amount of water transported by drain (mm ha^{-1}. Monthly)

3. Results

3.1. Projected changes in climatic indices

The weather series representing the near (2030–2059) and far (2070–2099) future, for each of the 11 GCM-RCM pairs were analysed and compared to the simulated control period (1983–2012) in combination with an analysis of the CFs for temperature and rainfall.

3.1.1. Temperature

Across all 11 model pairs and time-slices, mean temperature is projected to increase (Fig. 4). The highest annual increase is projected by RCMs driven by the HadCM GCM: +2.2 °C (+3.6 °C) in the near (far) future, and the lowest increase by combinations BCM-RCA and ECHAM-HIRHAM: $<$ +1.8 °C in the far future. The rest of the ensemble projects changes in the range of +2.0 to +2.6 °C in the far future. The temperature of the coldest and hottest day of the year (T_{cold} and T_{warm} respectively) also increases (Table A1, see Appendix), however the ECHAM-HIRHAM combination projects no change in the latter in the far future. As the temperature rises, the number of days with air frost decreases, and the date of the first air frost (in autumn), is predicted to occur later in the season by all 11 model experiments. In the near future the first air frost is projected to occur 9–26 days later, and in the far future 13–42 days later. Similarly, the date of the latest air frost (in spring) is projected to occur earlier in the season. In the near future the latest air frost will occur 5–22 days earlier, and in the far future 4–34 days earlier. A complete set of projected changes in the temperature and rainfall indices for each of the ensemble members is presented in Table A1 in the appendix.

Seasonal temperature and rainfall CFs are illustrated in Fig. 4 as uncertainty envelopes describing the range of the 11 climate model pairs. The ensemble mean is shown as a black dashed line. The near future change in mean temperature (Fig. 4a) shows no strong seasonal variation, but in the far future (Fig. 4b) increases are greater during winter, with a difference of ~1.0 °C for the ensemble mean between the changes in the winter and summer months. Furthermore, the two HadCM driven models (RCMs: CLM and HadRM) project noticeably higher temperature increases in both future periods, than the other 9 model combinations. This causes a larger spread of the ensemble predictions, especially during autumn and winter.

3.1.2. Rainfall

Annual rainfall is projected to increase in the future by 9 of 11 model combinations (Table A1). The projected changes range from −8% to +16% in the near future, and from −21% to +17% in the far future. The two Arpege driven combinations (RCMs: HIRHAM and RM5) project decreases, from -5% to −8% in the near future, and from −14% to −21% in the far future. The seasonal distribution of rainfall changes (Fig. 4), shows the same tendency as for temperature, where it is only for the far future that a seasonal pattern emerges with an associated increase in model uncertainty (indicated by the size of the envelope). The ensemble mean projects increased rainfall in the months from November to May, no change in June, July and October, and decreased rainfall in August and September. This decrease is largest in the Arpege combinations, which project a decrease in most months, which is strongest throughout spring, summer and autumn. Examining the projected changes in rainfall distribution of the Arpege combinations (hourly

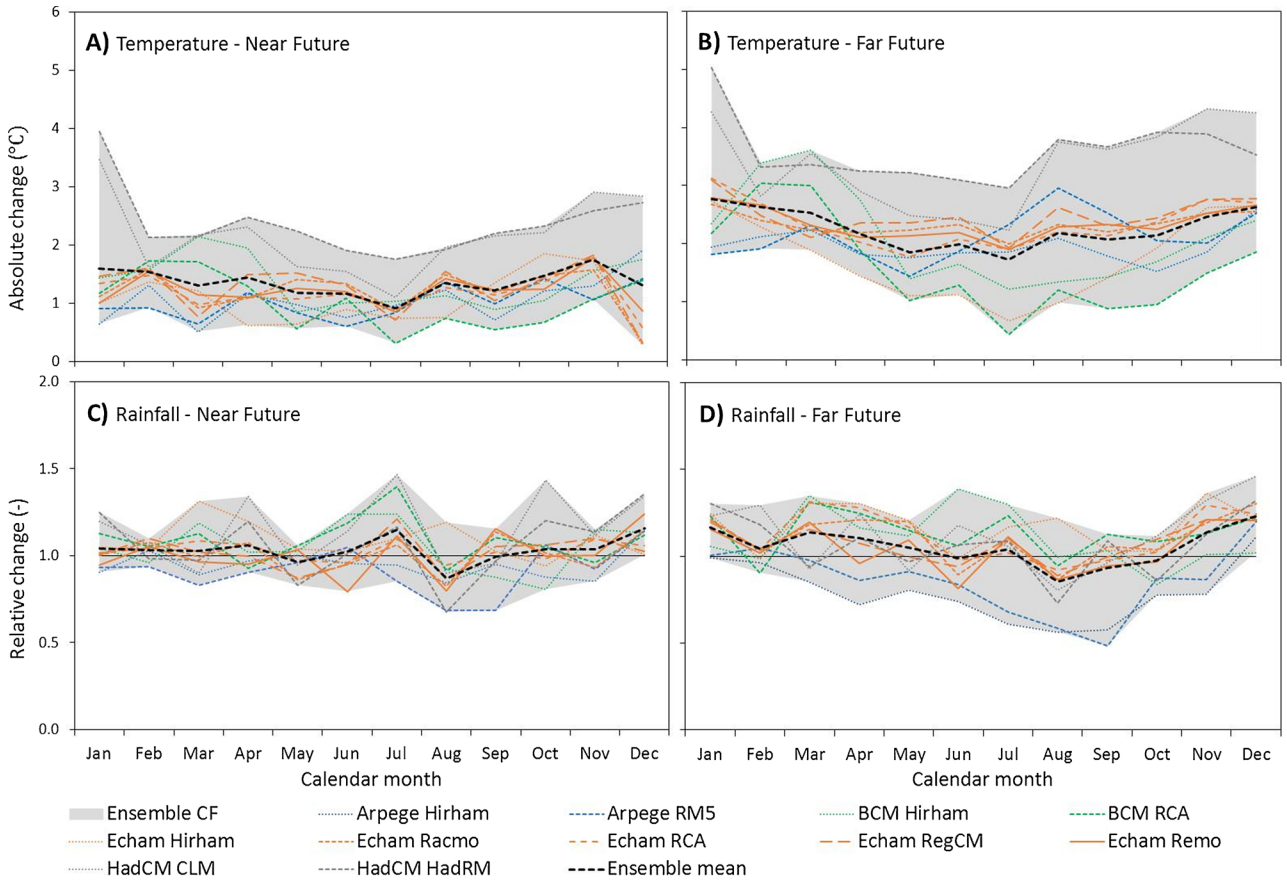

Fig. 4. Uncertainty envelope of monthly change factors for mean temperature and rainfall (temperature is given as absolute change and rainfall as relative change), for the near future (2030–2059) and far future (2070–2099). The solid horizontal line at 1.0 in C) and D) indicates 'no change'. RCMs driven by the same GCM are depicted by the same colour.

intensities from the simulated weather series) indicated that the decrease in annual rainfall (near and far future), was a result of fewer hours with a rainfall intensity in the range 1–3 mm/hour (low intensities) (results not shown) along with more zero rainfall hours.

Rainfall was downscaled to hourly resolution to evaluate indices of future changes in rainfall extremes (using Rmed − for definitions see Table 4) alongside indices for daily rainfall (wet days, SDII), and CFs (not shown) for rainfall statistics. The CFs for hourly rainfall projects an *annual* increase (by ensemble mean) in variance of 9% in the near future and 15% in the far future, in skewness of 3% and 5%, respectively. However, the range of projected changes indicates that increases and decreases are possible for these statistics, to the extent that strong seasonal patterns are not apparent. Except for July, the combination of fewer rain days (Table A1) in the summer months with a greater skewness, indicates that when it rains there is a greater risk of intense rainfall.

Apart from the Arpege models, all the models project an annual increase in the number of wet days, SDII, and R_{med} (Table A1). The projected changes in the *annual* number of wet days ranges from −4% to +23% in the near future, and from −23% to +21% in the far future. Corresponding changes in SDII range from increases of 1% to 10% in the near future, and from 2% to 13% in the far future; and changes in R_{med} range from −3% to +14% in the near future, and from −10% to +20% in the far future. The monthly distribution of these simulated control and future rainfall indices are shown in Fig. 5. The seasonal pattern in SDII, number of wet days, and R_{med} is clear, with the highest intensities during the summer months with a lesser, secondary peak during winter, especially for the number of wet days. The projected future *changes* do not show any consistent pattern, as the control simulation lies within the envelope in all months except for December and January for SDII and number of wet days, where all 11 model pairings agree that an increase will occur. This is consistent with the projected increases in winter rainfall illustrated in Fig. 4. The ensemble projection of extreme intensities indicated by R_{med} is associated with a higher degree of uncertainty during the summer months as the size of the envelope is generally greater in this period. This may reflect the uncertainties associated with the parameterization of convection within standard resolution RCMs and is a significant limitation in their use to assess changes in extreme sub-daily rainfall in mid-latitude summers (e.g. Ban et al., 2014; Chan et al., 2014).

3.2. Projected changes in agro indices

To evaluate indirect effects of future climatic changes on the conditions for crop production in Denmark, the soil-plant-atmosphere model Daisy was used to simulate simple crop sequences (winter wheat and silage maize), on 2 different soil types (coarse sand and sandy loam). Indirect effects were then evaluated in terms of crop development and as a consequence of potential changes in water shortage and excess.

3.2.1. Water excess: drainage and trafficability

It is assumed that water excess is not a problem on coarse sandy soils, due to the very high saturated hydraulic conductivity (Table 3). The water from heavy rainfall events usually rapidly infiltrates the soil and is transported to deeper soil layers, not restricting plant growth or traffic of farming machinery on the field. Hence, potential changes in the need for subsurface drainage and restrictions on trafficability is only evaluated on the sandy loam, which contains soil layers with low hydraulic conductivity and subsurface drains.

The amount of water (mm) transported away from the field by subsurface drains is illustrated in Fig. 6 (top panel), together with the

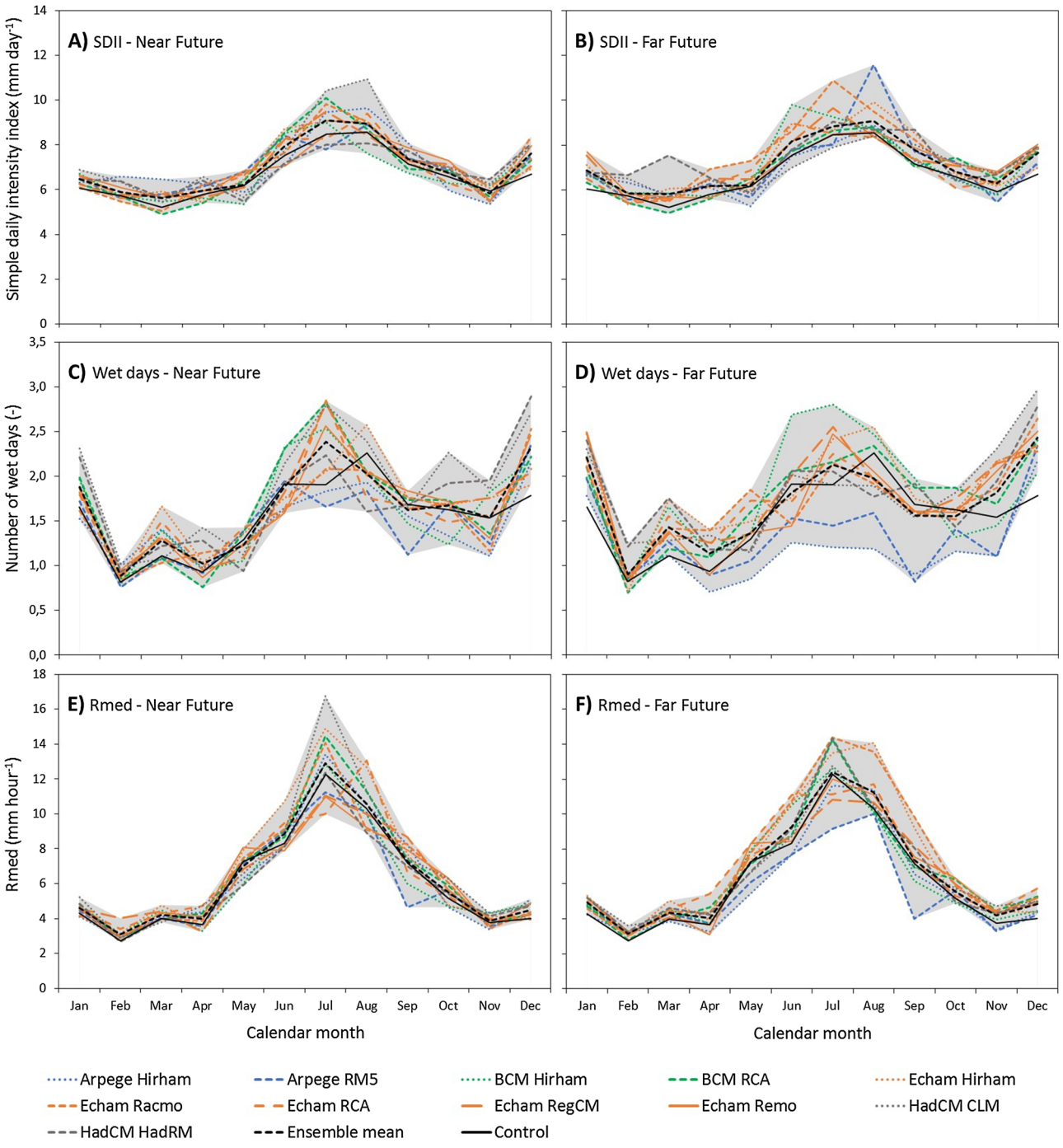

Fig. 5. Uncertainty envelope of simulated future rainfall indices. A and B, SDII; C and D, number of wet days; E and F, Rmed for each calendar month. The near future (2030–2059) is illustrated in the left column, and the far future (2070–2099) in the right column. The range of projections corresponding to the 11 climate model pairs is shown together with the ensemble mean and compared to the control simulation (1983–2012).

number of trafficable days (lower panel). Information on changes in average conditions has a value, but it is most often the variability in weather conditions that cause the greatest challenges for crop production, i.e. very wet or dry periods. To consider such potential extreme situations, which may have caused noticeable effects on agricultural conditions and/or practice, each year of the 3000-year simulations was ranked and the 96.7th percentile year for drainage flow and 3.3rd percentile year for the number of trafficable days (both illustrating particularly wet years) was evaluated. These percentiles correspond to the worst (wettest) event expected every 30-years (Fig. 6).

For such extreme years, a predictable seasonal effect on drain flow is seen, where it increases during autumn, peaks during winter, and decreases during spring and summer. The flow rate is least sensitive to climate model pairing between March and July, and most sensitive during autumn and winter. Uncertainty arising from climate model pairings increases when going from the near future to the far future, an increase which is largely caused by the Arpege combinations, especially in the winter months. Regarding future changes in extreme years, it is seen that the 9 ensemble members that project increased annual rainfall agree that the future drainage flow will increase during winter. The Arpege combinations however project decreased drainage flow in most months. Furthermore, the ensemble mean of extreme years shows an increase in drain flow occurring between August and October whilst the drains are typically inactive in this period in the extreme-year control

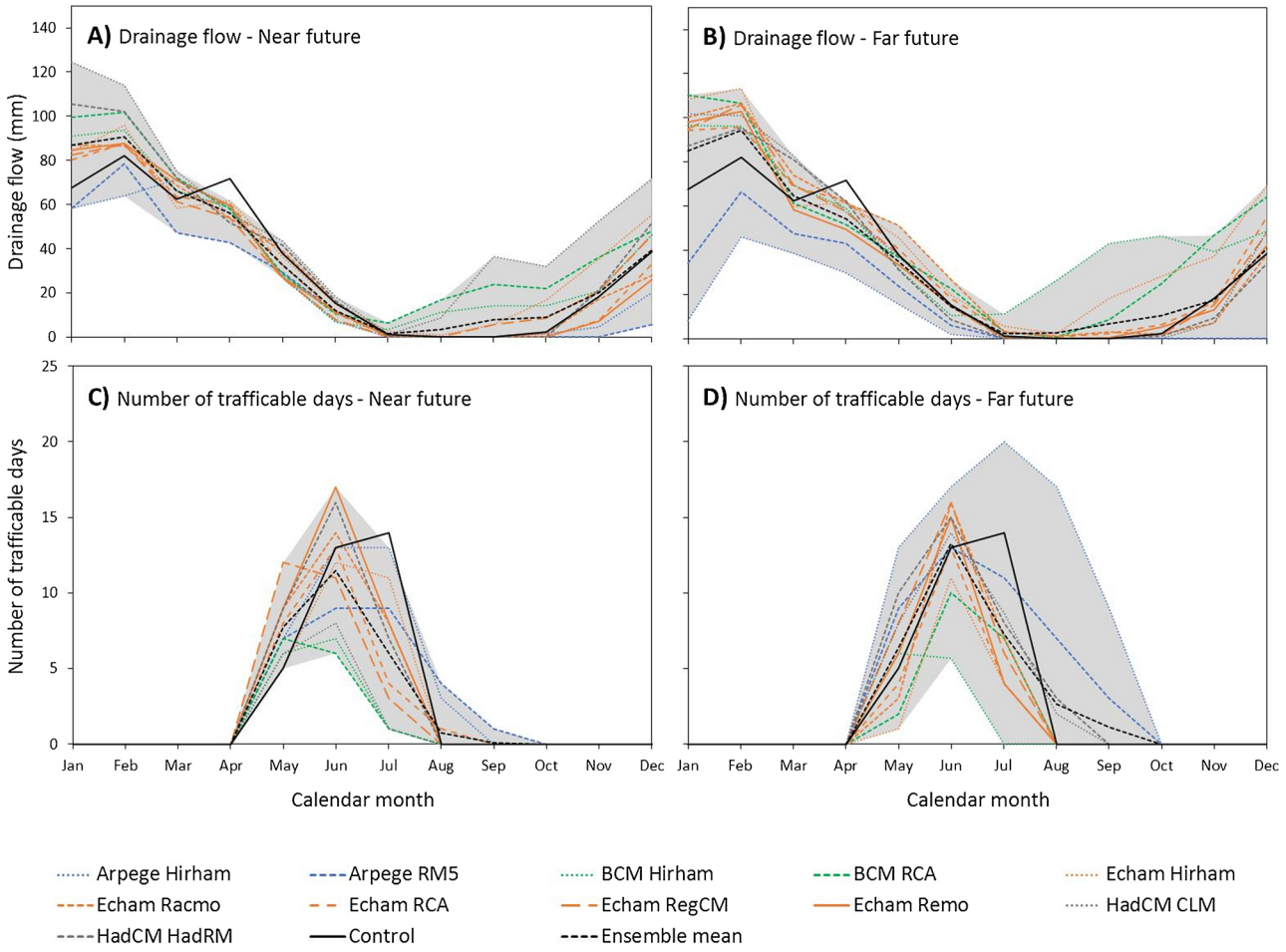

Fig. 6. Drainage flow and trafficability. Uncertainty envelope of future monthly drain flow (A and B), illustrated by the 96.7th percentile (wettest years), accompanied by number of trafficable days in the field (C and D), illustrated by the 3.3rd percentile (lowest number of trafficable days/wettest years). All simulated for the sandy loam soil. The near future (2030–2059) is illustrated in the left panel, and the far future (2070–2099) in the right panel. The range of results of the 11 climate model pairs is illustrated together with the ensemble mean and compared to the control simulation (1983–2012).

simulations. The water reserves of the soil are usually depleted after the higher summer temperatures, and have to be filled to activate a continuous drain flow (groundwater rise).

Comparing the extreme year future to control conditions, shows that the ensemble combinations project an change in the annual drainage flow ranging from −31% to +59% (ensemble mean of +7%), in the near future. In the far future, the projected change ranges from -65% to +45% (ensemble mean of +8%). In comparison, the mean drain flow (as opposed to the 96.7th percentiles representing extremely wet years) of the 3000 simulations, were projected to increase by an average of 10% (16%) in the near (far) future (Table A2).

Field trafficability is connected to the soil water content, as a large number of trafficable days occur during dry conditions. When considering the mean of the 3000 simulations, the field is more or less accessible at all times between May and August (results not shown), and the future changes are small. At an annual level, the ensemble mean projects the number of trafficable days to increase by 2 days (0.8%) in the near future and 10 days (3.0%) in the far future, an increase which is not expected to have significant effects on agricultural conditions.

This picture does not appear to change substantially when looking at the wettest years (at the 3.3rd percentile level) (Fig. 6A and B). The annual number of trafficable days has been projected to change from +4 to −18 days in the near future (ensemble mean of −6 days), and from +44 to −20 days in the far future (ensemble mean of −1 day). In the near future all models agree that the number of trafficable days will decline in July as this is the only month where the control simulations lie outside the projection envelope. In the far future the Arpege combinations predict an increase in number of trafficable days, increasing the model disagreement.

Hence, when looking at the mean of the 3000 simulations, overall a small increase in trafficable days are projected, whereas when looking at the years with the fewest trafficable days, a minor future reduction is projected. However, the magnitude of this reduction is relatively small compared with the annual total and so it is not expected to cause noticeable challenges.

3.2.2. Crop development

Analysis of the SM sowing date found no difference between the two soil types. However, the higher air temperatures illustrated in Fig. 4 resulted in higher soil temperatures earlier in the season. Consequently, the model ensemble projected SM to be sown 4–14 days earlier in the near future and 12–22 days earlier in the far future. The earlier sowing dates are indirectly related to the increased length of the potential growing season, which is projected to increase by 22–55 days, and 41–75 days, in the near and far future, respectively. The simulated harvest date of the two crops was highly affected by the projected climatic changes. All 22 future scenarios resulted in the crops ripening earlier in the future than in the control simulations, leading to an earlier harvest date. SM was especially affected as the crop was projected to be ready for harvest 22–53 days earlier in the near future, and 35–69 days, in the far future, for the sandy loam. SM ripened an additional 7 days earlier for both future periods for the coarse sand, whilst WW showed no dependence on soil type, and the ripening did not change as much as for SM. WW was

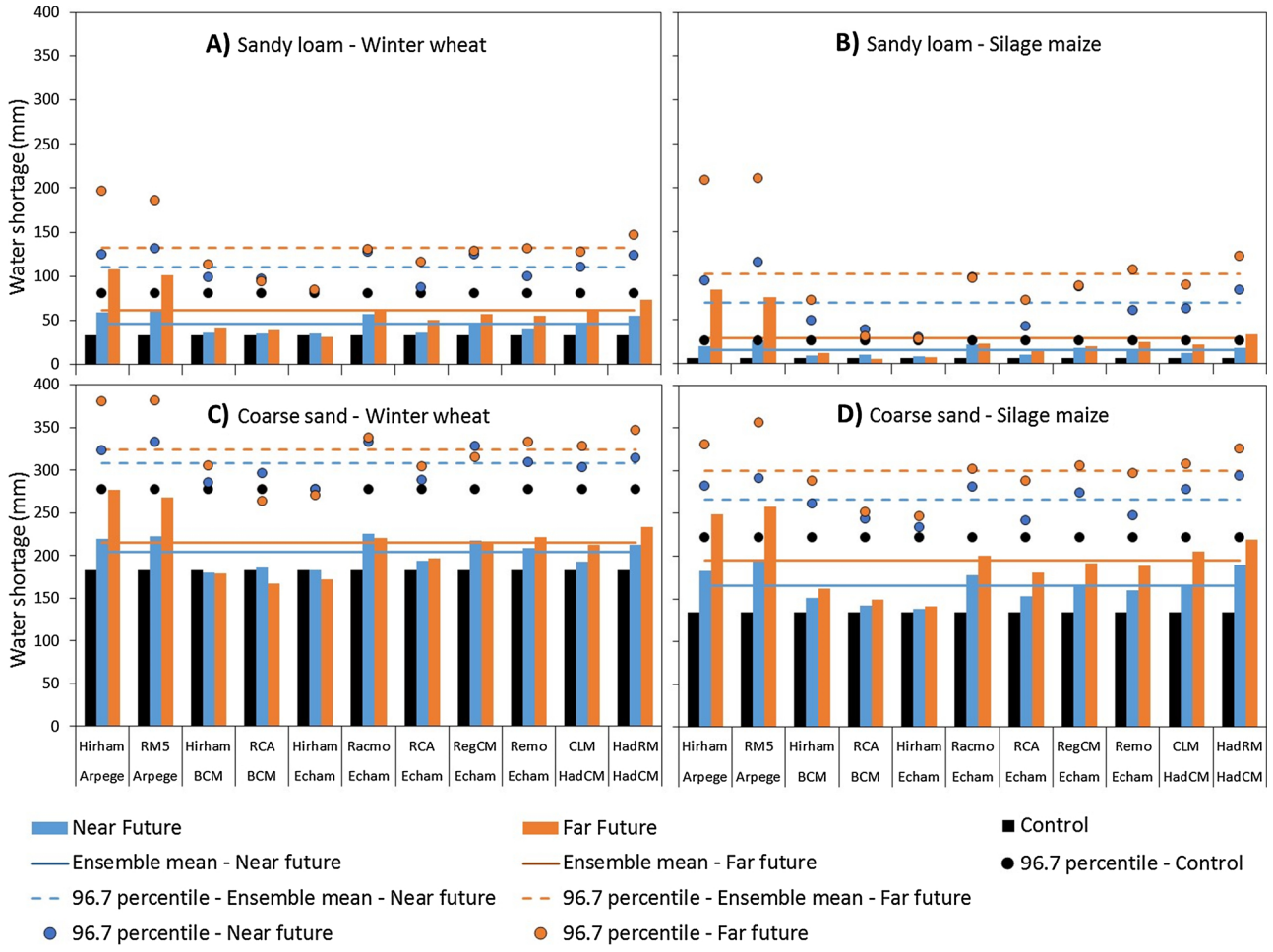

Fig. 7. Water shortage. Daisy simulations of near future (2030–2059) and far future (2070–2099) water shortage (potential evapotranspiration minus the actual evapotranspiration), of winter wheat and silage maize, for two soil types: sandy loam and coarse sand. Projections of the 11 climate model combinations are compared to the control period (1983–2012).

projected to be harvested 7–16 days earlier in the near future, and 10–21 days in the far future. These changes are related to the increased temperature causing the crops to ripen faster and so reducing the *active* growing season. A set of projected changes in agro indices is presented in Table A2 in the appendix.

3.2.3. Water shortage

The risk of future crop production being limited due to water stress is evaluated in terms of annual water shortage, here defined as annual ET_c minus ET_a, as simulated with Daisy. Most ensemble members show that the system will experience increased water shortage in the future, with a generally higher shortage in the far future than the near future (Fig. 7). The Arpege models project the greatest water shortage, and the BCM models together with the ECHAM-HIRHAM combination project the smallest changes compared to the control period. For the sandy loam, water shortage is relatively low (Fig. 7a and b). Under current conditions WW only experiences an average shortage of 33 mm, but future water shortage is projected to increase by an additional 2–27 mm, in the near future, and by 0–74 mm in the far future. The corresponding changes in water shortage for SM are only slightly smaller than those of WW (Table A2), however the absolute values are smaller (Fig. 7a and b). For the coarse sandy soil, the water shortage is higher, which is caused by differences between the two soils in water holding capacity and potential rooting depth. The sandy loam has a greater soil root zone capacity which is able to provide the crops with water to a higher degree than the coarse sandy soil. The absolute differences between the control and future periods (Fig. 7) are also greater than for the sandy loam. This is especially the case for SM which (compared to the control) experiences an increased annual water shortage of 3–62 mm (6–123 mm) in the near (far) future.

The impact of extreme years on crop water shortage is shown by the 96.7% percentile (approximately a 30 year event) in Fig. 7. Water shortage has generally increased, and so have the absolute changes from the control period (when looking at the ensemble mean). Although the changes are relatively small, the ensemble mean projects a greater increase in very dry years, compared to average years. The ensemble mean projected changes of water shortage in very dry years is practically identical between the soils whereas greater differences are found between the crops. The WW water shortage of very dry years are projected to increase by 30 mm in the near future at both soils, and 46 and 52 mm in the far future at the coarse sand and sandy loam, respectively. Whilst SM water shortage of very dry years are projected to increase by 44 mm in the near future at both soils, and 78 and 76 mm at the coarse sand and sandy loam, respectively.

3.2.4. Relative production

To investigate the level to which crop production is exploited (with respect to water supply), the simulations were repeated with the assumption that the crops do not suffer from water shortage. This means that the beneficial effect of an increased growing season is fully exploited, and the simulations represent a situation where all irrigation needs are satisfied. Comparing these simulations to those not receiving irrigation, gives an impression of potential beneficial effects of future irrigation and the term relative production is applied. The relative

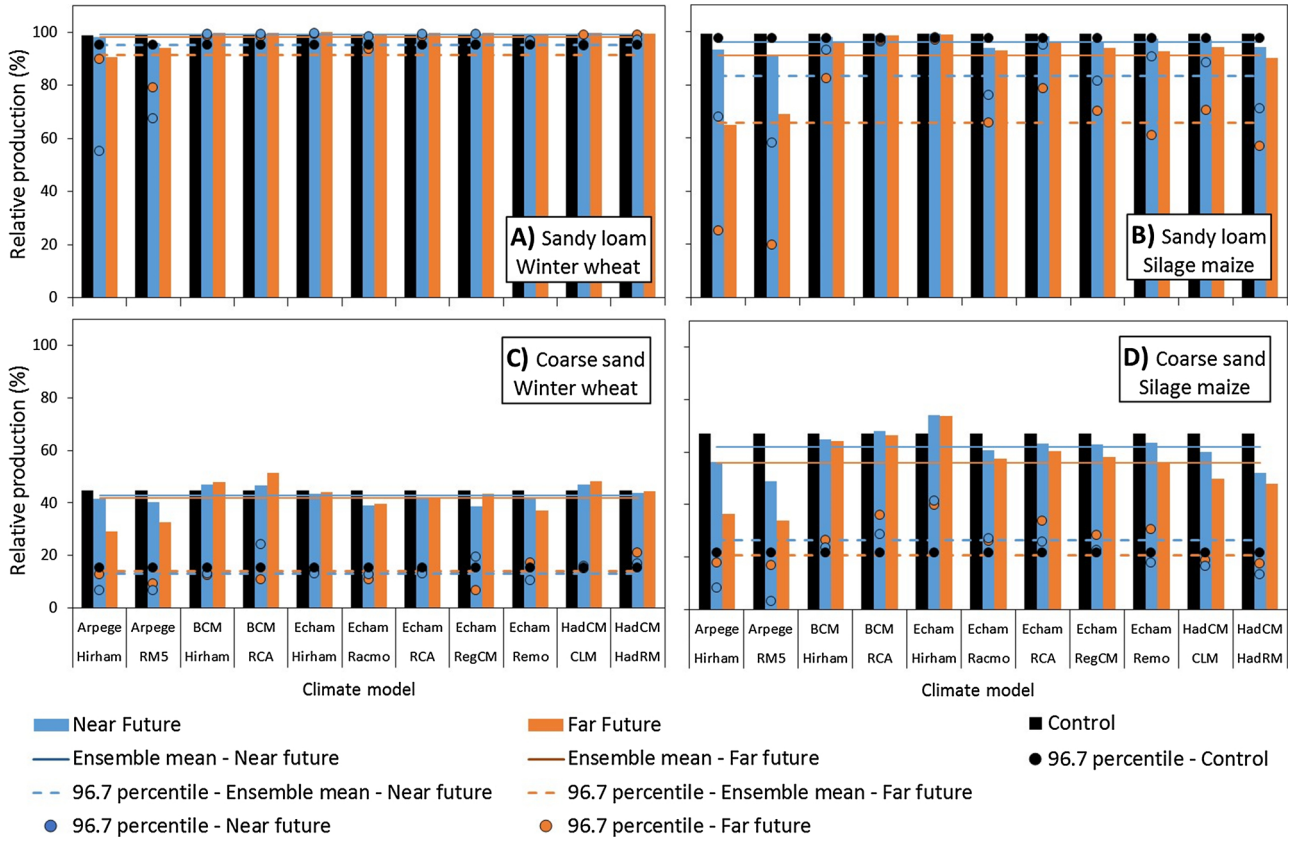

Fig. 8. Relative production. DAISY estimates of near future (2030–2059) and far future (2070–2099) relative production (crop yield, relative to yield when crops are fully irrigated, and growth is not limited by water shortage) of winter wheat and silage maize. Projections of the 11 climate model pairs are compared to results for the control period (1983–2012).

production is thus the ratio between water-limited production and potential production.

Under present (control) and future conditions, irrigating does not increase the yield of either WW and SM for the sandy loam, as the relative production predicted by the ensemble mean is close to 100% (Fig. 8a and b). The ensemble mean of the SM simulations resulted in 90% use of the production potential in the far future, although the two Arpege-driven combinations only projected 62–64% use of the production potential. This slight decrease in production potential for SM is likely a result of different growth periods. The growth of WW is mainly located in spring and early summer, whereas the growth of SM is located later in the season and thus responding to the generally projected decrease in summer rainfall.

For the coarse sandy soil (Fig. 8c and d), production is highly water limited under both current and future conditions, so it is beneficial to irrigate under current conditions as well as future. Regarding future conditions, the relative production of WW ranges from 39% to 47% in the near future, and from 29% to 51% in the far future. Corresponding values for SM are 49% to 74% in the near future and 34% to 74% in the far future. Compared to the control period, future simulations typically resulted in a lower relative production, as the WW control simulations reached a relative production of 45% and the SM simulations 67% (Fig. 8c and d). The slight decrease in relative production is expected to be a result of the reduced summer rainfall, which is especially evident for the Arpege driven RCMs. This means that the future need for irrigation for the coarse sandy soil is comparable to the present need, especially for WW where the exploitation of the production potential is only a few percentage-points lower in the future. However, it appears beneficial to increase the irrigation of SM in the future for coarse sandy soils, as the difference between the present and the future relative production is noticeably higher than for WW.

Each bar in Fig. 8 represents the mean of 3000 simulated years, which gives a robust indication of the projected increase or decrease in the relative production for each climate model pair. However, the distribution of annual results may be evaluated, which can give an indication of the vulnerability of crops to very dry years where irrigation might be very important to achieve acceptable yields. This vulnerability is again illustrated by the 3.3rd percentile of the relative production for each future period (Fig. 8), which corresponds roughly to a 30-year event. The control period relative production for the coarse sand is only 18% for WW and 21% for SM. For the sandy loam even very dry years do not indicate a need for irrigation in order to maintain yields, as the production potential for WW (SM) is 97% (98%).

Regarding future conditions, the simulations of WW for the sandy loam (Fig. 8a) generally (9 of 11 model combinations) show that the production potential in very dry years is very close to 100% and so relative production appears quite robust to future projections of change. Again, the two Arpege-driven simulations show a lower percentage of relative production for both soils. The very dry years in the SM simulations for the sandy loam (Fig. 8b) reaches a relative production ranging from 58% to 98% in the near future and from 20% to 97% in the far future. Comparing these values with the control period equivalent, a value of 98%, shows that in both future periods there is an increased risk of substantial SM yield losses in very dry years for sandy loam soils. For the coarse sandy soil the difference between the control and ensemble mean future projections are small. However, it cannot be concluded that the risk of very low crop yields will not change in the future, as the magnitude and direction of change is dominated by climate model uncertainty. The relative production of SM in particular was found to be more sensitive to climate model selection than that of WW.

Table 5
Annual CFs of mean temperature (absolute change, °C) and rainfall (relative change, non-dimensional) applied in the present study for the far future, 2070–2099 relative to the control period (1983–2012), compared to those found by Seaby et al. (2013).

GCM	RCM	Annual Δ			
		Temperature (°C)		Rainfall (−)	
		Present study Point scale	Seaby et al. (2013) National	Present study Point scale	Seaby et al. (2013) National
Arpege	HIRHAM	1.96	2.02	0.79	0.84
Arpege	RM5	2.14	2.07	0.86	0.89
BCM	HIRHAM	2.11	2.26	1.10	1.13
BCM	RCA	1.60	1.97	1.14	1.13
ECHAM	HIRHAM	1.74	1.92	1.17	1.19
ECHAM	RACMO	2.34	2.17	1.11	1.09
ECHAM	RCA	2.34	2.14	1.12	1.10
ECHAM	RegCM	2.48	2.29	1.08	1.07
ECHAM	Remo	2.35	2.14	1.05	1.06
HadCM	CLM	3.37	3.30	1.13	1.09
HadCM	HadRM	3.59	3.40	1.06	0.99
Ensemble mean		**2.26**	**2.34**	**1.05**	**1.05**

4. Discussion

4.1. Robustness of climate change signal

All 11 climate model combinations under the SRES A1B scenario for the future period of 2070–2099 project higher temperatures in the future, in the range of 1.6–3.6 °C annually (Table 5), which is supported by the general findings of other climate change studies (e.g. Doltra et al., 2014 and Seaby et al., 2013). The CFs evaluated for the present study are applied at a point scale, which allows the model projections to be used for climate change impacts assessments. The CFs are similar to those found by Seaby et al. (2013), also reported in Table 5, who calculated monthly CFs for all of Denmark, and used the same 11 model combinations from the ENSEMBLES project. However, Seaby et al. (2013) used a 20 year long control period (1991–2010) slightly different from the one applied in this study (1983–2013). It is demonstrated that the projected changes of each climate model downscaled to point scale (present study), are comparable to those at national level, as for the ensemble mean. Furthermore, the national CFs calculated by Seaby et al. (2013) also showed that the Arpege combinations projected an opposite, decreasing trend in mean rainfall to the ensemble mean.

Changes in extreme rainfall events, particularly those at sub-daily timescales are generally harder to project than changes in mean rainfall. Whilst output from RCMs are commonly available at daily resolution, few models provide readily available output at hourly resolution. Furthermore, RCMs have been noted to have severe limitations in reproducing the characteristics of sub-daily rainfall at resolutions coarser than ~10 km (Westra et al., 2014), including extremes, and studies over other regions have noted particularly limited skill in the simulation of summer rainfall extremes (Ban et al., 2014; Chan et al., 2014). We acknowledge therefore that the ensemble projections used here are limited in this regard. The emerging generation of very high resolution, convection-permitting climate models (Prein et al., 2015) has been shown to provide improved representation of short-duration convective extremes (e.g. Chan et al., 2014; Kendon et al., 2012) but few runs of these models have been conducted to date over limited spatial domains. This deficiency in standard resolution RCMs might offer some explanation as to why clear change in intense hourly rainfall is not apparent. Nonetheless, short, localized summer rainfall extremes may be of concern, hence, downscaling from the daily to hourly timescale was needed, which induces additional uncertainty. Although the resulting downscaled ensemble mean does not clarify whether there will be an increase or a decrease in the intensity of hourly extremes, the spread of model projections illustrates the potential for substantial changes to summer extremes.

Other studies have found an increased risk of future hourly extreme rainfall events (e.g. Arnbjerg-Nielsen, 2012), and high resolution modelling in other parts of Europe has suggested increases in intense summer rainfall (e.g. Kendon et al., 2014; Ban et al., 2014). Hence, it appears unwise to completely ignore the potential effects of extreme events on agricultural crop production and associated environmental impacts. Continued attention should be paid to developments in the provision of high resolution climate change scenarios. These may invalidate or offer improvements to the assumptions of stationarity in the relationship between daily and hourly rainfall changes, and could benefit future research into direct effects on e.g. lodging, erosion, and transport of agrochemicals to ground- and surface waters when planning future agricultural practices in Denmark.

The importance of applying ensemble modelling in agro-climatic impact studies is shown by the findings of the present study. 11 climate model combinations were investigated, and of these, 9 projected increased rainfall, whereas 2 projected a decrease. GCM selection has previously been found to be the primary driver in projections and their uncertainties (e.g. Prudhomme and Davies, 2009; Rowell, 2006), and although a full analysis of uncertainty has not been undertaken, the results here are consistent with this finding. Compared with the other climate model pairings, the Arpege driven pairs project a difference in direction of change in mean rainfall and the HadCM model pairs project substantially higher air temperatures.

4.2. Conditions for future crop production

The projected higher temperatures in the future result in a longer potential growing season (number of days per year with a daily average air temperature ≥ 5 °C). The growing season is prolonged on average by 30 days in the near future and 53 days in the far future. Not only does the growing season lengthen, but the date of the latest spring and earliest autumn frost also change in a way favourable for crop production in Denmark. A late spring frost is of particular agricultural importance as such an event occurring shortly after heading of WW may cause destruction of reproductive parts of the crop (Frederiks et al., 2015). Trnka et al. (2011) investigated future changes in the date of the last spring frost, and found changes comparable to those of the present study. The prolonged frost free period and higher temperatures stimulates plant growth. The detrimental effect of reduced active growing season on WW is found in other studies, and is often correlated with lower yields due to a reduced grain filling period (Kristensen et al., 2011; Olesen et al., 2000; Olesen et al., 2012). Here we do not focus on absolute yields (e.g. tonnes ha^{-1}), but it was found that WW yield for the sandy loam soil is projected to decrease by 2% in the near future, and 6% in the far future (results not shown). However, it has been proposed that the detrimental effects of climate change on WW may be overcome by use of other cultivars and technological development in management practice (Kristensen et al., 2011; Olesen et al., 2000). Furthermore, it has previously been shown that the detrimental effect on grain yields may be counterbalanced, or even surpassed, by the stimulating effect of increased CO_2 concentration on crop growth (Ghaffari et al., 2002). Changes in atmospheric CO_2 concentration were not included in this study, hence it can be expected that the predicted decrease in yields would be altered if CO_2 changes were included. Regarding the future need for irrigation, CO_2 is expected to have an effect, as the amount and size of stomatal openings have been found to decrease under elevated atmospheric CO_2 concentrations (Krujit et al., 2008). This reduces the evaporation, affecting the water balance to such an extent that increased water need caused by stimulated crop growth (increased leaf area index), may be counterbalanced (van Roosmalen et al., 2009).

The future production of maize in Scandinavian countries is considered to have great potential for increased production, as it was originally adapted to warmer climates than currently found in Scandinavia (Odgaard et al., 2011). Spring cereals, including maize, have been projected to be sown 1–2 weeks earlier in Denmark in the period 2031–2050 (Olesen et al., 2012), matching the results found in this study. As in this study, Olesen et al. (2012) based the simulated sowing dates only on temperature, hence disregarding the influence of wet soil conditions (trafficability), which is likely to affect the actual sowing date. As shown in Fig. 6, it is unlikely that the number of trafficable days will change noticeably in the future, which is also supported by Trnka et al. (2011). However, a potential move of the sowing date of maize and other spring cereals into March, may lead to problems with trafficability (Fig. 6c and d), as very few, if any, trafficable days are present in March. We do note though that the definition of a trafficable day is site specific, and it is more relevant to study the relative change than the absolute values. Nonetheless, placing the ideal sowing date earlier in the season increases the need of trafficable soil conditions in a period which is dominated by soil water recharge. Hence, the future need for drainage is likely to increase not only during the winter months, but also during early spring months.

If, as projected by 9 of 11 climate model-pairs, annual rainfall increases, the potential benefits of warmer weather will be supported by water supply. However, the seasonal rainfall distribution indicates that this extra rainfall may not occur at the right time for crop growth as it mainly falls during the winter months, before the silage maize is sown or whilst winter wheat is present but in a dormant state. Furthermore, the ensemble mean indicates a decrease in rainfall in spring and summer months in the far future, which may challenge the crop yields. The duration of the grain filling period is important, but maintaining a long period is only beneficial if droughts are avoided (Semenov et al., 2009). Comparing this information with the water shortage experienced by the crops in the future, it appears that a possible need for irrigation may occur, especially in the far future, and for coarse sandy soils cultivated with SM. This tendency is also reflected in the relative production, as irrigating SM has the greatest effects on the yield. The greater water need expressed by SM in the future most likely reflects the improved growing conditions (by means of temperature and radiation). SM yields for the sandy loam are projected to increase by 24% in both future periods, and for the coarse sand by 18% (12%) in the near (far) future, respectively (results not shown). These changes are high, but they are related to maize used for silage, hence the crop is not grown to full maturity. It is expected that the future climate can support the cultivation of corn maize in Denmark, allowing the utilization of maize to improve (Doltra et al., 2014; Kenny et al., 1993). Shifting from a production of silage maize to grain maize due to climate change, will most likely also include the use of other cultivars or varieties of maize. The current cultivars have relatively short growth periods, where farmers would most likely shift to cultivars of longer growth periods in the future. This will most likely further increase the future need for water on fields grown with maize, and a balance has to be found between long growth seasons and the consequent need for irrigation.

An average climatic year does not impose the need for irrigation, which is supported by the findings of Trnka et al. (2011), however a variation of irrigation needs is expected. Looking at the effect of very dry years on the relative production of SM, indicates a noticeable risk of decreased yields if SM is not irrigated (Fig. 8b). The projections also indicate an increased frequency of years which will require irrigation on sandy loam soils to ensure an acceptable SM yield, or at least to reach the potential of projected increased yields of SM. If, as projected by the Arpege driven ensemble members, annual rainfall decreases, the current water shortage on a sandy loam cultivated with SM will increase by 183–185 mm (approximately 25% of annual rainfall in Denmark).

It is not only the projected decrease in summer rainfall that may have consequences for crop production. The projected (ensemble mean) increases in autumn and winter rainfall suggest higher volumes of water will be transported away from the field by subsurface drains (a mean 10% increase in the near future, and 16% in the far future). The sandy loam used in these simulations does not have a large clay content, and agricultural crops grown on such soils may not be at risk of future water excess. However, agricultural soils containing more clay and/or located closer to ground water will probably experience even greater volumes of water transported by subsurface drains. It may be possible that existing drainage systems for such locations would have to be expanded, but this is left for future research.

5. Conclusions

Annual temperature is projected to increase by an ensemble of climate models, which results in a projected increased length of the potential growing season, earlier sowing, earlier ripening and harvest of crops. The spring sown crop silage maize particularly appears to benefit from the warmer climate, whereas the current cultivar of winter wheat shows negative responses to the projected climate change. A reduction of the active growing season results in a shortened grain filling period, which causes lower yields. Other cultivars are likely needed to overcome the potential detrimental climate effects on winter wheat production. If north European countries like Denmark are to benefit from the projected increase in production potential, there appear to be challenges in the form of increased risks of altered *conditions* for crop production that needs to be addressed:

- Water excess: The seasonal distribution of future rainfall suggests increased autumn and winter rainfall and decreased summer rainfall. However, the ensemble models project changes which point in different directions as well as magnitudes, which means that great uncertainties are associated with the projections. Following the ensemble mean, an increased water excess will occur during winter, resulting in a mean 10% increase in drainage water in the near future, and 16% in the far future.
- Water shortage: The decreased summer rainfall results in increased need for irrigation, especially for SM cultivated on coarse sandy soils. But, in extremely dry years (30 year events), even WW cultivated in sandy loam soils, may need additional irrigation. This irrigation need relates to the achievement of the production potential, as especially SM yield in the coarse sandy soil will respond positively if irrigated in the future.
- Extreme rainfall: There was no climate model consensus as to the direction of change of extreme hourly rainfall intensity. However, the uncertainty arising from the climate model choice indicated changes of up to +30% in the magnitude of R_{med}, with the greatest absolute changes being in the summer months.

Funding

Funding was provided by University of Copenhagen. Stephen Blenkinsop was supported by the INTENSE project, funded by the European Research Council (grant ERC-2013-CoG-617329).

Acknowledgements

We thank the Danish Meteorological Institute (DMI) for supplying daily observed weather data, and The Water Pollution Committee of The Society of Danish Engineers (DWPCC) for supplying the hourly observed rainfall data. Furthermore, we acknowledge the ENSEMBLES project database for providing simulated future weather series.

Appendix A

Tables A1 (climatic indices) and Table A2(agronomic indices), on the following pages, gives an overview of annual projected changes for all investigated indices.

Table A1
Projected annual mean future changes in *climatic* indices. The change is provided for each index from the control period (1983–2012) to the projected near future (NF: 2030–2059) and far future (FF: 2070–2099). When the change is absolute, the unit is given in parenthesis, and where the change is relative the change is given by percentage.

GCM–RCM	Temperature and rainfall indices																							
	Annual mean T (°C)		Tcold (°C)		Twarm (°C)		Date of first air frost (days)		Date of latest air frost (days)		Number of frost days per year (days)		Length of growing season (days)		Annual rainfall (%)		SDII (%)		Number of rain days (%)		Number of wet days (%)		Rmed (%)	
	NF	FF	NF	FF	NF	FF	NF	FF	NF	FF	NF	FF	NF	FF	NF	FF	NF	FF	NF	FF	NF	FF	NF	FF
Arpege–HIRHAM	+1.1	+2.0	+0.4	+2.2	+1.4	+2.4	+15	+19	−7	−4	−19	−36	+23	+41	−5	−21	+6	+2	−9	−21	−4	−23	+2	−4
Arpege–RM5	+1.1	+2.3	+0.4	+2.3	+1.1	+3.7	+12	+20	−7	−13	−18	−36	+22	+42	−8	−14	+5	+6	−11	−16	−4	−12	−3	−10
BCM–HIRHAM	+1.4	+2.1	+2.1	+3.9	+0.7	+1.0	+12	+20	−18	−34	−32	−48	+35	+55	+6	+11	+1	+7	+4	+4	+7	+17	+1	+5
BCM–RCA	+1.1	+1.7	+2.2	+4.0	+0.2	+0.7	+9	+13	−11	−23	−29	−46	+28	+47	+8	+13	+3	+3	+4	+10	+10	+14	+8	+9
ECHAM–HIRHAM	+1.1	+1.8	+1.5	+3.4	+0.2	+0.0	+18	+30	−5	−14	−21	−43	+22	+50	+8	+17	+5	+8	+4	+9	+10	+21	+14	+18
ECHAM–Racmo	+1.3	+2.4	+1.4	+3.5	+1.4	+2.8	+16	+24	−10	−19	−20	−43	+22	+49	+0	+9	+5	+13	−4	−1	+1	+13	+5	+20
ECHAM–RCA	+1.3	+2.4	+1.9	+4.4	+0.9	+2.5	+16	+28	−9	−19	−24	−49	+24	+55	+3	+11	+3	+5	+1	+7	+6	+13	+5	+14
ECHAM–RegCM	+1.3	+2.6	+1.7	+3.8	+1.2	+3.1	+15	+24	−10	−17	−21	−44	+24	+51	+3	+8	+5	+9	−3	0	+8	+16	+2	+7
ECHAM–Remo	+1.3	+2.4	+1.6	+3.4	+1.1	+2.2	+16	+23	−8	−18	−21	−43	+24	+50	+1	+5	+5	+8	−4	−3	+7	+12	+3	+8
HadCM–CLM	+2.2	+3.4	+2.8	+4.4	+1.6	+3.6	+26	+42	−22	−28	−42	−56	+53	+75	+16	+11	+10	+6	+4	+5	+23	+17	+14	+7
HadCM–HadRM	+2.4	+3.6	+3.6	+4.8	+1.9	+4.1	+24	+35	−21	−32	−45	−55	+55	+72	+6	+6	+4	+12	+2	−4	+12	+17	−1	+10
Ensemble mean	+1.4	+2.4	+1.8	+3.6	+1.1	+2.4	+16	+25	−12	−21	−27	−46	+30	+53	+3	+5	+5	+7	−1	−1	+7	+10	+5	+8

Table A2
Projected annual mean future changes in *agricultural* indices. The change from the control period (1983–2012) to the projected near future (NF: 2030–2059) and far future. (FF: 2070–2099). When the change is absolute the unit is given in parenthesis, and where the change is relative the change is given by percentage.

GCM–RCM	Agricultural indices–Sandy loam									
	Sowing date of silage maize (days)		Harvest date of silage maize (days)		Harvest date of winter wheat (days)		Crop water shortage–silage maize (mm)		Crop water shortage–winter wheat (mm)	
	NF	FF	NF	FF	NF	FF	NF	FF	NF	FF
Arpege–HIRHAM	−6	−14	−27	−51	−7	−16	+13	+78	+26	+74
Arpege–RM5	−6	−16	−29	−55	−7	−15	+19	+69	+27	+68
BCM–HIRHAM	−11	−19	−33	−51	−10	−15	+3	+6	+3	+7
BCM–RCA	−8	−13	−22	−35	−8	−12	+3	0	+2	+5
ECHAM–HIRHAM	−4	−12	−27	−39	−7	−10	+1	0	+2	0
ECHAM–Racmo	−8	−16	−36	−56	−11	−18	+15	+16	+24	+29
ECHAM–RCA	−5	−15	−31	−52	−9	−16	+4	+8	+2	+17
ECHAM–RegCM	−9	−16	−37	−57	−11	−18	+11	+13	+13	+23
ECHAM–Remo	−7	−16	−33	−55	−10	−17	+7	+18	+6	+22
HadCM–CLM	−14	−22	−49	−65	−13	−16	+6	+15	+11	+27
HadCM–HadRM	−13	−21	−53	−69	−16	−21	+12	+26	+22	+40
Ensemble mean	−8	−16	−34	−53	−10	−16	+9	+22	+13	+28

(*continued on next page*)

Table A2 (*continued*)

GCM–RCM	Agricultural indices–Sandy loam								Agricultural indices–Coarse sand			
	Relative production–silage maize (%)		Relative production–winter wheat (%)		Drainage flow (%)		Trafficability (days)		Harvest date of silage maize (days)		Harvest date of winter wheat (days)	
	NF	FF	NF	FF	NF	FF	NF	FF	NF	FF	NF	FF
Arpege–HIRHAM	−6	−34	−1	−8	−31	−79	+18	+58	−17	−43	−7	−16
Arpege–RM5	−9	−30	−3	−5	−43	−58	+25	+41	−23	−39	−7	−15
BCM–HIRHAM	−2	−3	+1	+1	+19	+47	−7	−19	−27	−43	−10	−15
BCM–RCA	−1	−1	0	+1	+39	+73	−13	−13	−18	−27	−8	−12
ECHAM–HIRHAM	0	0	+1	+1	+34	+79	−9	−16	−23	−35	−7	−10
ECHAM–Racmo	−5	−6	−1	+1	0	+39	+3	+9	−27	−49	−11	−18
ECHAM–RCA	−1	−4	+1	+1	−2	+47	+4	−3	−28	−45	−9	−16
ECHAM–RegCM	−4	−5	0	+1	+4	+29	−4	+4	−31	−49	−11	−18
ECHAM–Remo	−2	−7	0	0	−7	+15	+6	+5	−30	−51	−9	−17
HadCM–CLM	−2	−5	+1	+1	+81	+31	−7	+20	−43	−62	−13	−16
HadCM–HadRM	−5	−9	+1	+1	+28	+9	+11	+25	−46	−66	−16	−21
Ensemble mean	−3	−10	0	−1	+10	+16	+2	+10	−28	−46	−10	−16

GCM–RCM	Agricultural indices–Coarse sand							
	Crop water shortage–silage maize (mm)		Crop water shortage–winter wheat (mm)		Relative production–silage maize (%)		Relative production–winter wheat (%)	
	NF	FF	NF	FF	NF	FF	NF	FF
Arpege–HIRHAM	+48	+114	+36	+94	−11	−31	−3	−16
Arpege–RM5	+62	+123	+39	+85	−18	−33	−4	−12
BCM–HIRHAM	+17	+27	−4	−5	−2	−3	+2	+3
BCM–RCA	+7	+14	+2	−16	+1	−1	+2	+6
ECHAM–HIRHAM	+3	+6	0	−12	+7	+7	−1	−1
ECHAM–Racmo	+43	+66	+42	+37	−7	−10	−6	−5
ECHAM–RCA	+19	+46	+11	+13	−4	−7	−3	−3
ECHAM–RegCM	+31	+57	+35	+31	−4	−9	−6	−1
ECHAM–Remo	+26	+54	+26	+38	−4	−11	−3	−8
HadCM–CLM	+30	+71	+9	+29	−7	−18	+2	+3
HadCM–HadRM	+55	+84	+29	+50	−15	−19	−1	0
Ensemble mean	+31	+60	+20	+31	−6	−12	−2	−3

References

Andreasen, M., Andreasen, L.A., Jensen, K.H., Sonnenborg, T.O., Bircher, S., 2013. Estimation of regional groundwater recharge using data from a distributed soil moisture network. Vadose Zone J. 12.

Arnbjerg-Nielsen, K., 2012. Quantification of climate change effects on extreme precipitation used for high resolution hydrologic design. Urban Water Des. 9, 57–65.

Aslyng, H.C., 1978. Vanding I Jordbruget. DSR Forlag, Den Kgl. Veterinær- Og Landbohøjskole.

Asseng, S., et al., 2014. Rising temperatures reduce global wheat production. Nat. Clim. Change 5, 143–147.

Ban, N., Schmidli, J., Schär, C., 2014. Evaluation of the convection-resolving regional climate modeling approach in decade-long simulations. J. Geophys. Res. 119, 7889–7907.

Boegh, E., Thorsen, M., Butts, M., Hansen, S., Christiansen, J.S., van der Keur, P., Refsgaard, J.C., Schelde, K., Soegaard, H., Thomsen, A., 2004. Incorporating remote sensing data in physically based distributed agro-hydrology modelling. J. Hydrol. 287, 279–299.

Böhm, U., Kücken, M., Ahrens, W., Block, A., Hauffe, D., Keuler, K., Rockel, B., Will, A., 2006. CLM—the climate version of LM: brief description and long-term applications. COSMO Newslett. 6 (5).

Burton, A., Kilsby, C.G., Fowler, H.J., Cowpertwait, P.S.P., O'Connell, P.E., 2008. RainSim: a spatial-temporal stochastic rainfall modelling system. Environ. Model. Softw. 23, 1356–1369.

Burton, A., Fowler, H.J., Kilsby, C.G., O'Connell, P.E., 2010. A stochastic model for the spatial-temporal simulation of nonhomogeneous rainfall occurrence and amounts. Water Resour. Res. 46.

Challinor, A.J., Watson, J., Lobell, D.B., Howden, S.M., Smith, D.R., Chhetri, N., 2014. A meta-analysis of crop yield under climate change and adaptation. Nat. Clim. Change 4, 287–291.

Chan, S.C., Kendon, E.J., Fowler, H.J., Blenkinsop, S., Roberts, N., Ferro, C.A.T., 2014. The value of high-resolution Met Office regional climate models in the simulation of multi-hourly precipitation extremes. J. Clim 27, 6155–6174.

Christensen, O.B., Drews, M., Christensen, J.H., Dethloff, K., Ketelsen, K., Hebestadt, I., Rinke, A., 2006. The HIRHAM regional climate model version 5, Danish Meteorological Institute Technical Report 06-17. Danish Meteorological Institute, Copenhagen.

Collins, M., Booth, B.B.B., Harris, G.R., Murphy, J.M., Sexton, D.M.H., Webb, M.J., 2006. Towards quantifying uncertainty in transient climate change. Clim. Dyn. 27, 127–147. https://doi.org/10.1007/s00382-006-0121-0.

Cowpertwait, P.S.P., O'Connel, P.E., Metcalfe, A.V., Mawdsley, J.A., 1996. Stochastic point process modelling of rainfall. II. Regionalisation and disaggregation. J. Hydrol. 175, 47–65.

DWPCC, 2016. The Water Pollution Committee of The Society of Danish Engineers. https://universe.ida.dk/netvaerk/energi-miljoe-og-global-development/spildevandskomiteen/regnmaalerstyregruppen/.

Déqué, M., Dreveton, C., Braun, A., Cariolle, D., 1994. The ARPEGE/IFS atmosphere model: a contribution to the French community climate modelling. Clim. Dyn. 10, 249–266. https://doi.org/10.1007/BF00208992.

Doltra, J., Lægdsmand, M., Olesen, J.E., 2014. Impacts of projected climate change on productivity and nitrogen leaching of crop rotations in arable and pig farming systems in Denmark. J. Agric. Sci. 152, 75–92.

EEA, 2017. Climate Change, Impacts and Vulnerability in Europe 2016. An Indicator-based Report. European Environment Agency, Luxembourg.

Easterling, W.E., Aggarwal, P.K., Batima, P., et al., 2007. Food, fibre and forest products. Climate change 2007: impacts, adaptation and vulnerability. Contribution of Working Group II. In: Parry, M.L., Canziani, O.F., Palutikof, J.P., van der Linden, P.J., Hanson, C.E. (Eds.), The Fourth Assessment Report of the Intergovernmental Panel on Climate Change. Cambridge University Press, Cambridge, pp. 273–313.

Elsgaard, L., Børgesen, C.D., Olesen, J.E., Siebert, S., Ewert, F., Peltonen-Sainio, P., Rötter, R.P., Skjelvåg, A.O., 2012. Shifts in comparative advantages for maize, oat, and wheat cropping under climate change in Europe. Food Addit. Contam. 29, 1514–1526.

FAO, 1986. Irrigation Water Management: Irrigation Water Needs. FAO, Rome.

FAO, 2015. Statistical Pocketbook. Food and Agriculture Organization of the United Nations, Rome, pp. 2015.

Flury, M., 1996. Experimental evidence of transport of pesticides through field soils –a review. J. Environ. Qual. 25, 25–45.

Frederiks, T.M., Christopher, J.T., Sutherland, M.W., Borrell, A.K., 2015. Post-head-emergence frost in wheat and barley: defining the problem, assessing the damage, and identifying resistance. J. Exp. Bot. 66, 3487–3498.

Gerke, H.H., Arning, M., Stöppler-Zimmer, H., 1999. Modelling long-term compost application effects on nitrate leaching. Plant Soil 213, 75–92.

Ghaffari, A., Cook, H.F., Lee, H.C., 2002. Climate change and winter wheat management: a modelling scenario for south-eastern England. Clim. Change 55, 509–533.

Gjettermann, B., Styczen, M., Hansen, H.C.B., Vinther, F.P., Hansen, S., 2008. Challenges in modelling dissolved organic matter dynamics in agricultural soil using DAISY. Soil Biol. Biochem. 40, 1506–1518.

Gobin, A., 2010. Modelling climate impacts on crop yields in Belgium. Clim. Res. 44, 55–68.

Grass, R., Thies, B., Kersebaum, K., Wachendorf, M., 2015. Simulating dry matter yield of two cropping systems with the simulation model HERMES to evaluate impact of future climate. Eur. J. Agron. 70, 1–10.

Håkansson, I., Keller, T., Arvidsson, J., Rydberg, T., 2012. Effects of seedbed properties on crop emergence. 5. Effects of aggregate size, sowing depth and simulated rainfall after sowing on harmful surface-layer hardening. Acta Agric. Scand. Sec. B −Soil Plant Sci. 62, 362–373.

Hansen, S., Jensen, H.E., Nielsen, N.E., Svendsen, H., 1991. Simulation of nitrogen dynamics and biomass production in winter wheat using the Danish simulation model Daisy. Fertil. Res. 27, 245–259.

Hansen, S., Abrahamsen, P., Petersen, C.T., Styczen, M., 2012. Daisy Model use, calibration, and validation. Am. Soc. Agric. Biol. Eng. 55, 1315–1333.

IPCC, 2014. In: Core Writing Team, Pachauri, R.K., Meyer, L.A. (Eds.), Climate Change 2014: Synthesis Report. Contribution of Working Groups I, II and III to the Fifth Assessment Report of the Intergovernmental Panel on Climate Change. IPCC, Geneva, Switzerland.

Jacob, D., et al., 2001. A comprehensive model inter-comparison study investigating the water budget during the BALTEX-PIDCAP period. Meteorol. Atmos. Phys. 77 (1–4), 19–43. https://doi.org/10.1007/s007030170015.

Jacobsen, O.H., (1989), Unsaturrated hydraulic conductivity in some Danish soils. Vol. S-2030. In Danish. Crop research of the Danish Government, Copenhagen.

Jones, R., Hassell, D., Hudson, D., Wilson, S., Jenkins, G., Mitchell, J., 2003. Generating high resolution climate change scenarios using PRECIS. UNDP National Communications Unit Workbook. 34 pp.

Jones, P.D., Kilsby, C.G., Harpham, C., Glenis, V., Burton, A., 2009. UK Climate Projections Science Report: Projections of Future Daily Climate for the UK from the Weather Generator. University of Newcastle, UK ISBN 978–1-906360–06-1. http://ukclimateprojections.defra.gov.uk.

Jones, P.D., Harpham, C., Burton, A., Goodess, C.M., 2016. Downscaling regional climate model outputs for the Caribbean using a weather generator. Int. J. Clim. 36, 4141–4163. https://doi.org/10.1002/joc.4624.

Kendon, E.J., Roberts, N.M., Senior, C.A., Roberts, M.J., 2012. Realism of rainfall in a very high resolution regional climate model. J. Clim. 25, 5791–5806.

Kendon, E.J., Roberts, N.M., Fowler, H.J., Roberts, M.J., Chan, S.C., Senior, C.A., 2014. Heavier summer downpours with climate change revealed by weather forecast resolution model. Nat. Clim. Change 4, 570–576.

Kenny, G.J., Harrison, P.A., Olesen, J.E., Parry, M.L., 1993. The effects of climate change on land suitability of grain maize, winter wheat and cauliflower in Europe. Eur. J. Agron. 2, 325–338.

Kilsby, C.G., Jones, P.D., Burton, A., Ford, A.C., Fowler, H.J., Harpham, C., James, P., Smith, A., Wilby, R.L., 2007. A daily weather generator for use in climate change studies. Environ. Model. Softw. 22, 1705–1719.

Kjaer, J., Ernstsen, V., Jacobsen, O.H., Hansen, N., de Jonge, L.W., Olsen, P., 2011. Transport modes and pathways of the strongly sorbing pesticides glyphosate and pendimethalin through drained soils. Chemosphere 84, 471–479.

Kjellström E., Bärring L., Gollvik S., Hansson U., Jones C., Samuelsson P., Rummukainen M., Ullersig A., Willen U., Wyser K. (2005), A 140-year simulation of European climate with the new version of the Rossby Centre regional atmospheric climate model (RCA3). Reports meteorology and climatology, 108, SMHI, SE-60176 Norrkoping, Sweden, 54 pp.

Kloss, S., Pushpalatha, R., Kamoyo, K.J., Schütze, N., 2012. Evaluation of crop models for simulating and optimizing deficit irrigation systems in arid and semi-arid countries under climate variability. Water Resour. Manag. 26, 997–1014.

Kristensen, K., Schelde, K., Olesen, J.E., 2011. Winter wheat yield response to climate variability in Denmark. J. Agric. Sci. 149, 33–47.

Krujit, B., Witte, J.P.M., Jacobs, C.M.J., Kroon, T., 2008. Effects of rising atmospheric CO2 on evapotranspiration and soil moisture: a practical approach for the Netherlands. J. Hydrol. 349, 257–267.

Manevski, K., Børgesen, C.D., Andersen, M.N., Kristensen, I.S., 2015. Reduced nitrogen leaching by intercropping maize with red fescue on sandy soils in North Europe: a combined field and modelling study. Plant Soil 388, 67–85.

Martin, M.M., Olesen, J.E., Porter, J.R., 2014. A genotype, environment and management (GxExM) analysis of adaptation in winter wheat to climate change in Denmark. Agric. For. Meteorol. 187, 1–13.

Mela, T.J.N., 1996. Northern agriculture: constraints and responses to global climate change. Agric. Food Sci. Finland 3, 229–234.

Mollerup, M., Abrahamsen, P., Petersen, C.T., Hansen, S., 2014. Comparison of simulated water, nitrate, and bromide transport using a Hooghoudt based and a dynamic drainage model. Water Resour. Res. 50, 1080–1094.

Murphy, J.M., Sexton, D.M.H., Barnett, D.N., Jones, G.S., Webb, M.J., Collins, M., Stainforth, D.A., 2014. Quantification of modelling uncertainties in a large ensemble of climate change simulations. Nature 430, 768–772.

Niu, L., Feng, S., Ding, W., Li, G., 2016. Influence of speed and rainfall on large-scale wheat lodging from 2007 to 2014 in China. PLoS One 11.

Odgaard, M.V., Bøcher, P.K., Dalgaard, T., Svenning, J.C., 2011. Climatic and non-climatic drivers of spatiotemporal maize-area dynamics across the northern limit for maize production –a case study from Denmark. Agric. Ecosyst. Environ. 142, 291–302.

Olesen, S.E., 2009. Kortlægning af potentielt dræningsbehov på landbrugsarealer opdelt efter landskabselement, geologi, jordklasse, geologisk region samt høj/lavbund. DJF, Intern rapport. Markbrug nr. 21.

Olesen, J.E., Jensen, T., Petersen, J., 2000. Sensitivity of field-scale winter wheat production in Denmark to climate variability and climate change. Clim. Res. 15, 221–238.

Olesen, J.E., Jabobsen, B.H., Thorup-Kristensen, K., Andersson, N., Kudsk, P., Jørgensen, L.N., Hansen, L.M., Nielsen, B.L., Boelt, B., (2006), Tilpasning til klimaændringer i landbrug og havebrug. DJF rapport, Markbrug nr. 128. In Danish.

Olesen, J.E., Børgesen, C.D., Elsgaard, L., Palouso, T., Rötter, R.P., Skjelvåg, A.O., Peltonen-Sainio, P., Börjesson, T., Trnka, M., Ewert, F., Siebert, S., Brisson, N., Eitzinger, J., van Asselt, E.D., Oberforster, M., van der Fels-Klerx, H.J., 2012. Changes in time of sowing, flowering and maturity of cerials in Europe under climate change.

Food Addit. Contam. 29, 1527–1542.
Olesen, M., Madsen, K.S., Ludwigsen, C.A., Boberg, F., Christensen, T., Cappelen, J., Christensen, O.B., Andersen, K.K., Christensen, J.H., 2014. Fremtidige Klimaændringer I Danmark. Danmarks Klimacenter Rapport. DMI.
Otterå, O.H., Bentsen, M., Bethke, I., Kvamstø, N.G., 2009. Simulated pre-industrial climate in Bergen Climate Model (version 2): model description and large-scale circulation features. Geosci. Model Dev. 2, 197–212. https://doi.org/10.5194/gmd-2-197-2009.
Pal, J., et al., 2007. Regional climate modeling for the developing world: the ICTP RegCM3 and RegCNET. Bull. Am. Meteorol. Soc. 88, 1395–1409. https://doi.org/10.1175/BAMS-88-9-1395.
Palosuo, T., Kersebaum, K.C., Angulo, C., Hlavinka, P., Moriondo, M., Olesen, J.E., Patil, R.V., Ruget, F., Rumbaur, C., Takac, J., Trnka, M., Bindi, M., Caldag, B., Ewert, F., Ferrise, R., Mirschel, W., Saylan, L., Siska, B., Rötter, R., 2011. Simulation of winter wheat yield and its variability in different climates of Europe: a comparison of eight crop growth models. Eur. J. Agron. 35, 103–114.
Panagos, P., Ballabio, C., Borrelli, P., Meusburger, K., Klik, A., Rousseva, S., Tadic, M.P., Michaelides, S., Hrabalikova, M., Olsen, P., Aalto, J., Lakatos, M., Rymszewicz, A., Dumitrescu, A., Begueria, S., Alewell, C., 2015. Rainfall erosivity in Europe. Sci. Total Environ. 511, 801–814.
Patil, R.H., Laegdsmand, M., Olesen, J.E., Porter, J.R., 2012. Sensitivity of crop yield and N losses in winter wheat to changes in mean and variability of temperature and precipitation in Denmark using the FASSET model. Acta Agric. Scand. Sec. B −Soil Plant Sci. 62, 335–351.
Porter, J.R., Xie, L., Challinor, A.J., Cochrane, K., Howden, S.M., Iqbal, M.M., Lobell, D.B., Travasso, M.I., 2014. Food security and food production systems. In: Field, C.B., Barros, V.R., Dokken, D.J., Mach, K.J., Mastrandrea, M.D., Bilir, T.E., Chatterjee, M., Ebi, K.L., Estrada, Y.O., Genova, R.C., Girma, B., Kissel, E.S., Levy, A.N., MacCracken, S., Mastrandrea, P.R., White, L.L. (Eds.), Climate Change 2014: Impacts, Adaptation, and Vulnerability. Part A: Global and Sectoral Aspects. Contribution of Working Group II to the Fifth Assessment Report of the Intergovernmental Panel on Climate Change. Cambridge University Press Cambridge, United Kingdom and New York, NY, USA.
Prein, A.F., Langhans, W., Fosser, G., Ferrone, A., Ban, N., Goergen, K., Keller, M., Tölle, M., Gutjahr, O., Feser, F., et al., 2015. A review on regional convection-permitting climate modelling Demonstrations, prospects, and challenges. Rev. Geophys. 53, 323–361.
Prudhomme, C., Davies, H., 2009. Assessing uncertainties in climate change impacts analyses on the river flow regimes in the UK. Part 2: future climate. Clim. Change 93, 197–222.
Prudhomme, C., Reynard, N., Crooks, S., 2002. Downscaling of global climate models for flood frequency analysis: where are we now? Hydrol. Process 16, 1137–1150.
R. Radu, M. Déqué, S. Somot, (2008), Spectral nudging in a spectral regional climate model, Tellus Ser. A 60(5), 898–910, 10.1111/j.1600-0870.2008.00341.x.
Rasmussen, S.B., Abrahamsen, P., Nielsen, M.H., Holm, P.E., Hansen, S., 2015. Effects of single rainfall events on leaching of glyphosate and bentazone on two different soil types, using the Daisy model. Vadose Zone J. 14.
Reyer, C.P.O., Leuzinger, S., Ramming, A., Wolf, A., Bartholomeus, R.P., Bonfante, A., Lorenzi, F., Dury, M., Gloning, P., Jaoude, R.A., Klein, T., Kuster, T.M., Martins, M., Niedrist, G., Riccardi, M., Wohlfahrt, G., Angelis, P., Dato, G., Francois, L., Menzel, A., Pereira, M., 2013. A plant́s perspective of extremes: terrestrial plant responses to changing climatic variability. Glob. Change Biol. 19, 75–89.
Roeckner E., Bäuml G., Bonaventura L., Brokopf R., Esch M., Giorgetta M., Hagemann S., Kirchner I., Kornblueh L., Manzini E., Rhodin A., Schlese U., Schulzweida U., Tompkins A. (2003), The atmospheric general circulation model ECHAM5. Part I: model description. Max Planck Institute for Meteorology Rep. 349. Available from MPI for Meteorology, Bundesstr 53, 20146 Hamburg, Germany, 127 pp.
Rowell, D.P., 2006. A demonstration of the uncertainty in projections of UK climate change resulting from regional model formulation. Clim. Change 79, 243–257.
Schneider, S.H., 1983. CO_2, climate and society: a brief overview. In: Chen, R.S., Boulding, E., Schneider, S.H. (Eds.), Social Science Research and Climate Change: in Interdisciplinary Appraisal. D. Reidel Boston, MA, USA.
Seaby, L.P., Refsgaard, J.C., Sonnenborg, T.O., Stisen, S., Christensen, J.H., Jensen, K.H., 2013. Assessment of robustness and significance of climate change signals for an ensemble of distribution-based scaled climate projections. J. Hydrol. 486, 479–493.
Semenov, M.A., Martre, P., Jamieson, P.D., 2009. Quantifying effects of simple wheat traits on yield in water-limited environments using a modelling approach. Agric. For. Meteorol. 149, 1095–1104.
Svendsen, H., Hansen, S., Jensen, H.E., 1995. Simulation of crop production, water and nitrogen balances in two German agro-ecosystems using the Daisy model. Ecol. Model. 81, 197–212.
Trnka, M., Olesen, J.E., Kersebaum, K.C., Skjelvåg, A.O., Eitzinger, J., Seguin, B., Peltonen-Sainio, P., Rötter, R., Iglesias, A., Orlandini, S., Dubrovsky, M., Hlavinka, P., Balek, J., Eckersten, H., Cloppet, E., Calanca, P., Gobin, A., Vucetic, V., Nejedlik, P., Kumar, S., Lalic, B., Mestre, A., Rossi, F., Kozyra, J., Alexandrov, V., Semeradova, D., Zalud, Z., 2011. Agroclimatic conditions in Europe under climate change. Glob. Change Biol. 17, 2298–2318.
van der Linden, P., Mitchell, J.F.B. (Eds.), 2009. ENSEMBLES: Climate Change and Its Impacts: Summary of Research and Results from the ENSEMBLES Project. Met Office Hadley Centre, FitzRoy Road, Exeter EX1 3PB, UK.
Van Meijgaard E., van Ulft L.H., van de Berg W.J., Bosveld F.C., van den Hurk B.J.J.M., Lenderink G., Siebesma A.P. (2008), The KNMI regional atmospheric climate model RACMO, version 2.1. KNMI publication: TR-302, 43 pp.
van Roosmalen, L., Sonneborg, T.O., Jensen, K.H., 2009. Impact of climate and land use change on the hydrology of a large-scale agricultural catchment. Water Resour. Res. 45.
Vanuytrecht, E., Raes, D., Willems, P., Semenov, M.A., 2014. Comparing climate change impacts on cereal based on CMIP3 and EU-ENSEMBLES climate scenarios. Agric. For. Meteorol. 195, 12–23.
Watts, M., Goodess, C.M., Jones, P.D., 2004. The CRU Daily Weather Generator. BETWIXT Technical Briefing Note 1, Version 2. (February).
Westra, S., Fowler, H.J., Evans, J.P., Alexander, L.V., Berg, P., Johnson, F., Kendon, E.J., Lenderink, G., Roberts, N.M., 2014. Future changes to the intensity and frequency of short-duration extreme rainfall. Rev. Geophys. 52, 522–555.
Zhao, C., et al., 2017. Temperature increase reduces global yields of major crops in four independent estimates. Proc. Nat. Acad. Sci. 114, 9326–9331.